Supporting information for

Are soybean models ready for climate change food impact assessments?

Kritika Kothari[1], Rafael Battisti[2], Kenneth J. Boote[3], Sotirios V. Archontoulis[4], Adriana Confalone[5], Julie Constantin[6], Santiago V. Cuadra[7], Philippe Debaeke[6], Babacar Faye[8], Brian Grant[9], Gerrit Hoogenboom[3,10], Qi Jing[9], Michael van der Laan[11], Fernando Antônio Macena da Silva[7], Fabio R. Marin[12], Alireza Nehbandani[13], Claas Nendel[14], Larry C. Purcell[15], Budong Qian[9], Alex C. Ruane[16], Céline Schoving[6], Evandro H.F.M. Silva[12], Ward Smith[9], Afshin Soltani[13], Amit Srivastava[8], Nilson A. Vieira Jr.[12], Stacey Slone[18], Montserrat Salmeron[1*]

Contents

SI1. Source of weather data

Weather data for Ames, Iowa were obtained from the Iowa Mesonet website (https://mesonet.agron.iastate.edu/agclimate/hist/hourly.php), which included temperature and precipitation data from NWS COOP Station (AMES-8-WSW) and wind speed and humidity data from Iowa State University AgClimate Network Station (Ames-AEA, Boone County). For Auzeville, France, data from a weather station at the experimental site were obtained from the INRAE centralized climate data system in France (CLIMATIK). For Azul, Argentina, we obtained solar radiation, temperature, and rainfall data from the weather station located at the experimental field in the Faculty of Agronomy, Azul, Buenos Aires, for the 1988–2010 period; and from the Azul station of the National Meteorological Service, located 1000 m from the experimental field, for the 1980–1987 period. We extracted wind speed and humidity variables for Azul, Argentina from the AgMERRA dataset. For Fayetteville, Arkansas, temperature and precipitation data came from a weather station of the Global Historical Climatology Network (Menne et al., 2012), and missing values were filled with station-bias adjusted AgMERRA data. Wind speed, humidity, and solar radiation variables at Fayetteville, Arkansas were taken from the AgMERRA data. For Brasilia, Brazil, the data were obtained from the Embrapa Cerrados weather station, located 200 m from experimental site. This station is registered in the HIDRO database of the National Water Agency – ANA (http://www.snirh.gov.br/hidroweb/apresentacao) as: CPAC-Main Station, Code: 01547016.

SI2. Description of model calibration

APSIM

The **APSIM** v9 parameters changed from *Blind* to *Full* calibration are provided in Supplementary Table 10 per environment. The temperature and [CO_2] response functions affecting rates of crop processes in the model (Supplementary Tables 7 and 8) remained unchanged between *Blind* to *Full* calibration. However, the changes in some other model coefficients during calibration related to cultivar specific phenology and growth parameters affected the yield response to temperature and [CO_2].

In Arkansas, no parameters were changed since *Blind* calibration resulted in satisfactory performance. In Argentina, we used generic phenology parameters of maturity group (MG) 3.5 in *Blind* but switched to MG 5.0 in *Full* calibration. We increased the RUE values from default of 0.88 g MJ^{-1} (during emergence to end of grain filling) and 0.44 g MJ^{-1} (during end grain filling to maturity) to 0.92 g MJ^{-1} across all stages. Fraction of dry matter allocated to pod was slightly decreased. The "svp" parameter that affects evapotranspiration (ET) and water demand, was decreased from 0.75 to 0.65. This is consistent with a previous maize exercise in Iowa (Kimball et al., 2019) in which that change helped in simulating daily ET. This change improved the simulation of the rainfed treatments in this study. In Brazil, RUE parameter was increased from 0.88 and 0.44 g MJ^{-1} (stage dependent) to 1.00 g MJ^{-1} across stages. Plant density error was corrected from *Blind* to *Full* calibration (10 to 40 plants m^{-2}) for the late planting. In France, phenological parameters were changed from MG 1.5 to MG 1. The RUE parameters were increased from 0.44 to 0.88 g MJ^{-1} across stages. Fraction of dry matter allocated to pod was slightly decreased. The "svp" parameter decreased from 0.75 to 0.65. In Iowa, soil water model was changed from SoilWat to SWIM, to enable simulation of water table dynamics and best represent actual growing conditions, and match soil water measurements.

In general, in the study the majority of changes in the APSIM model were related to cultivar phenological parameters and RUE. An important aspect that came up in two environments was the simulation of yields under water-limited conditions (underestimation). This could be due to either crop or soil parametrization. The solution that followed in this exercise was to lower the "svp" parameter that affects ET and water demand. This change is consistent and agrees with a recent maize ET exercise (Kimball et al., 2019) in which the maize svp was decreased. This is something to be further investigated.

AQUACROP

The AQUACROP model v.6.1 simulates the effect of the environment and management on crop production. The model has two types of crop parameters: (i) conservative parameters, no need to calibrate because these are valid for all cultivars in all environments, and (ii) cultivar specific parameters, these are affected by field management, planting mode, soil profile conditions, and climate-related parameters. These parameters were estimated following the procedures developed by Steduto et al. (2012). The parameters related to crop response to temperature, including upper and lower cardinal temperatures for crop development (5°C and 30°C) and pollination (8°C and 40°C), were not changed during calibration. Similarly, the parameters related to [CO_2] effect on crop response, including normalized biomass-water productivity (WP* = 15 g m^{-2}), remained the same between the calibration steps.

During *Blind* calibration, we calibrated parameters related to developmental stages to match the observed phenology. The parameters included time to 90% seedling emergence, time to reach maximum canopy cover, time to beginning of canopy senescence, time to physiological maturity, time to start of flowering, and duration of flowering.

During *Full* calibration, parameters related to canopy development, Harvest Index, and soil water holding traits were modified to match in-season growth. The values of key crop parameters are summarized in Supplementary Table 10. Canopy growth coefficient (CGC) and canopy decline coefficient (CDC) were adjusted for all sites. Reference harvest index was increased for all sites except Argentina. Maximum effective rooting depth was increased in Arkansas, Brazil, and France.

DNDC

The calibration approach for the DNDC model is focused on the adjustment of the generic cultivar parameters available for each crop type which are provided in Supplementary Table 10. The model does not include the characterization of cultivar-specific cultivars in the framework but instead expects the user to tweak the generic crop parameters for a given crop type to meet the cultivar-specific characteristics. The [CO_2] response was calibrated before *Blind* calibration to ensure it was in line with the current literature reported [CO_2] response values but was not adjusted between *Blind* and *Full* calibration. The optimal temperature for each cultivar-location was correlated to the location growing season average temperature and set for both steps in an optimal range of 25.8–29ºC. No other temperature related responses were adjusted for the calibration steps.

During the *Blind* calibration step, the crop parameters that were adjusted included maximum percentage of carbon in grain, leaf/stem/root/grain fractions, leaf/stem/root/grain carbon to nitrogen ratio, cumulative degree days (TDD), optimum temperature, water requirement, biological N-fixation, rooting depth. These parameters were either adopted from previous validation studies with DNDC or, when feasible, fit to best match the provided phenological data provided in the initial *Blind* calibration step. Soil characteristics were not modified from the data provided for each site location.

For the *Full* calibration step the crop parameters were further refined to match observed yield and harvest index values through adjustment of maximum grain carbon, leaf/stem/root/grain fractions, water requirement and further adjustment of grain carbon to nitrogen ratio and water requirement was carried out to improve fits to nitrogen uptake and soil water extraction.

DSSAT CSM-CROPGRO-Soybean

The cultivar parameters that were calibrated in the **CSM-CROPGRO-Soybean model within DSSAT** are given in Supplementary Table 10. No parameters relevant to the rate of response of different plant processes in response to temperature (Supplementary Table 8) were calibrated, thus the responses of growth to temperatures were expected to be similar between the *Blind* and *Full* calibration steps for this model. Likewise, no parameters related to crop processes responses to [CO_2] responses were calibrated.

During the *Blind* calibration to optimize the simulated compared to observed timing of reproductive stages, the cultivar coefficients for development were calibrated, including CSDL, PPSEN, EM-FL, FL-SH, FL-SD, and SD-PM. We started with the DSSAT's default cultivars for MG 2 (for France), 3 (Iowa), 4 (Arkansas & Argentina), and 6 (Brazil).

For the *Full* calibration, the parameters LFMAX, SLAVR, WTPSD, SFDUR, PODUR, THRSH, FL-LF, and FL-VS relevant to soybean vegetative and reproductive growth were calibrated. Some reproductive development parameters were further modified during *Full* calibration to improve fit to pod and seed growth. In the calibration phase, soil parameters were also modified for two sites. For Argentina, the SRGF at depth was increased and the DUL was increased and the initial conditions were modified to match the early soil water measurements. For France, the soil was poorly parameterized initially, therefore during *Full* calibration the SAT was increased by 0.04, the drainage rate SLDR was reduced from 0.7 to 0.5, and rooting (SRGF) was increased by 0.01 for the bottom layer, No modifications of soils were made for Arkansas or Brazil or Iowa.

DSSAT Energy Balance (EBL) CSM-CROPGRO-Soybean

The cultivar parameters in the **CSM-CROPGRO-Soybean model in Energy Balance** mode within DSSAT are presented in Supplementary Table 10. Parameters related to temperature and [CO_2] response are similar to that of DSSAT classic version (Supplementary Table 8), and they were not modified during *Blind* or *Full* calibration. Therefore, the yield and growth response to changes in temperature or [CO_2] are expected to be similar between the *Blind* and *Full* calibration.

During the *Blind* calibration, we started with cultivars calibrated from the DSSAT classic version, which were built on default cultivars for MG 2 (France), 3 (Iowa), 4 (Arkansas & Argentina), and 6 (Brazil). We then optimized the developmental stages by further calibrating parameters EM-FL, FL-SD, SD-PM, FL-LF. The CSDL and PPSEN parameters for DSSAT-EBL version were the same as that of the classic version.

For the Full calibration, the parameters related to vegetative and reproductive growth were calibrated including LFMAX, SLAVR, WTPSD, SFDUR, PODUR, THRSH, FL-LF, and SIZLF. Some phenological parameters were re-adjusted to match the seed and pod growth data. The differences between cultivar coefficients of DSSAT-EBL and classic DSSAT versions were greater for Arkansas and Iowa compared to the other locations. Similar to DSSAT classic version, the soil parameters were modified for two sites. For Argentina, the SRGF at depth was increased and the DUL was increased and the initial conditions were modified to match the early soil water measurements. For France, the SAT was increased by 0.04, the drainage rate SLDR was reduced from 0.7 to 0.5, and rooting (SRGF) was increased by 0.01 for the bottom layer. No modifications of soils were made for Arkansas or Brazil or Iowa.

LINTUL

The cultivar parameters for LINTUL5 are given in Supplementary Table 10. No parameters related to crop processes response to temperature and [CO_2] (Supplementary Table 10) were altered from *Blind* to *Full* calibration, except for France. In France *Full* phase, the relative rate of RUE with average daily temperature (TMPFTB) was modified to add a failure temperature threshold of 50°C, and the reduction factor of RUE as function of lower minimum temperature (TMNFTB) was reduced from 3 to -20°C.

In the *Blind* phase, we calibrated coefficients related to phenology including TSUMEM, TSUM1, and TSUM2 to match the development phases (Supplementary Table 10). For other parameters, we used default values, which were common for all locations.

For *Full* calibration, parameters RGRLAI and SLATB were modified to match the LAI, parameters related to partitioning (FRTB, FLTB, FSTB, and FOTB), and RUETB were changed to match in-season growth. Some development parameters were re-adjusted in accordance with in-season growth data. For France, additional parameters including LAICR, KDIFTB, RDRL, RDRSHM, RRI, DVSDR, and DVSDLT were modified to simulate water stress effect between treatments. Maximum rooting depth was also changed to match soil water observations. The fraction of crop nitrogen uptake by biological fixation (NFIXF) was calibrated from 0.8 (*Blind*) to 0.7 (*Full)*.

MONICA

The simulation model for nitrogen and carbon dynamics in agro-ecosystems (**MONICA**) has five groups of parameters, including files of crops, crop-residues, general, mineral-fertilizers and organic-fertilizers (Nendel et al., 2011a; Specka et al., 2015). The calibration was performed mainly in crops file that included species and cultivars parameters. The species are in most case not changed, including parameters related with base temperature for development and assimilation, nitrogen (concentration, uptake, biological fixation, responses to deficit), initial organ biomass, initial rooting depth, organ growth and maintenance respiration, root penetration rate and specific root length. The cultivar file had 13 parameters (the total number of parameters is 32) to be calibrated (Battisti et al., 2017a). The MONICA model considers seven crop stages: sowing to emergence; emergence to end of juvenile phase; end of juvenile phase to flower appearance; flower appearance to first pod; first pod to last pod; last pod to harvest maturity; and senescence.

During *Blind* calibration, parameters of thermal time (adjusted to reduce error) and photoperiod sensitivity (obtained based on the default values by cultivar maturity group) were changed.

The *Full* calibration phase was done to adjust biomass and yield level. The parameters calibrated were root depth, maximum assimilation rate, specific leaf area and biomass partitioning (growth and senescence). The parameters used in the *Blind* and *Full* calibration are shown in Supplementary Table 10. Thermal time was also adjusted in the *Full* calibration (MONICA has an effect of water deficit on life cycle, because changes in the parameters related with that and limiting information about some crop phases, changes about crop phases were done), but in a soft way to adjust pod growth time.

The root depth parameter was reduced from 150 cm to 100 cm to reduce water available to the crop. The cultivar parameter of maximum assimilation rate or maximum photosynthesis rate was reduced about 15% to reduce total biomass. The specific leaf area parameter was reduced during *Full* calibration because of high LAI. We increased partition to root before the start of pod growth to reduce aboveground biomass, we increased partition to stem after the start of pod growth to reduce yield, and increased leaf senescence after the start of seed growth to reduce LAI late in the cycle.

No parameters related to the temperature and [CO_2] response functions of different crop processes were adjusted between *Blind* and *Full* calibration. Still, some changes in the temperature response curve occurred over 30°C in the sensitivity analysis for MONICA, probably associated with a plateau response of rate of development to temperatures above 25-30°C (Supplementary Table 8). In contrast, the rate of RUE decreases with temperature above 36°C. This means that development continued at a maximum rate as air temperature increased, while the rate of photosynthesis was reduced with temperatures above 36°C.

SSM

In SSM-Soybean cardinal temperatures for rate of development and RUE (Supplementary Table 8) are species-dependent and remained unchanged during *Blind* and *Full* calibration. The same is true for the response of RUE and transpiration coefficient to [CO_2] concentration.

During *Blind* calibration, the parameters bdSOWEMR, bdEMRR1, bdR1R3, bdR3R5, bdR5R7, bdR7R8, CPP, ppsen, Phyl and PLAPOW were changed (Supplementary Table 10). During *Full* calibration, parameters IRUE, FLF1A, FLF1B, FRTRL, PDHI, EED, WSSG, WSSL, WSSD, WSSN, GNCmin, GNCmax and MXNUP were changed.

STICS

The cultivar parameters that were calibrated in the STICS model are given in table S10. Parameters governing the rate of response of different processes to temperature were not modified during the calibration exercise, thus the responses of growth to temperatures were expected to be similar between the *Blind* and *Full* calibration steps. Likewise, no parameters related to the response of crop processes to [CO_2] were calibrated.

During the *Blind* calibration to optimize the simulated compared to observed reproductive stages, the cultivar coefficients for development were calibrated, and they remained the same for the *Full* calibration.

For the *Full* calibration, the parameters efcroijuv, efcroiveg, and efcroirepro related to RUE; the parameters dlaimaxbrut and durvieF relevant to leaf growth; nbjgrain and cgrain relevant to reproductive growth; and vitircarbT controlling harvest index were changed. In addition for France, parameters pertaining to biological N2 fixation, vitno and fixmax, were modified.

SWB

The cultivar parameters that were calibrated in the **SWB** are given in Supplementary Table 10. Definitions for these parameters can be found in Annandale et al. (2000). Parameters related to the rate of response of different plant processes to temperature remained unchanged during the calibration steps, thus the responses of growth to temperatures were expected to be similar between the *Blind* and *Full* calibration steps. Likewise, parameters related to [CO_2] effect on crop processes were not modified during calibration.

During the *Blind* calibration, we started with a set of default cultivar parameters (Jovanovic et al., 2002) for all locations, and then to match the observed developmental stages, we calibrated the cultivar coefficients for phenology, including degree days to emergence, flowering and maturity.

For the *Full* calibration, the parameters specific leaf area (SLA), leaf senescence degree days, RUE, total dry matter at emergence, leaf-stem partitioning, stem to grain translocation, dry matter to water ratio and extinction coefficient relevant to soybean vegetative and reproductive growth were calibrated. The RUE was reduced in Arkansas and Iowa, while it was increased at other sites. SLA was increased for all sites except France where it was reduced, and degree days to leaf senescence were advanced at Brazil and Argentina. Some development parameters were further modified during *Full* calibration to improve fit to pod and seed growth at two sites, including reducing emergence degree days for Argentina and France, flowering duration increased at Argentina, and maturity delayed at France. In the *Full* calibration, root parameters were also modified for all sites to match soil water measurements. Maximum rooting depth was increased for Arkansas, Argentina, and Brazil, and reduced for Iowa. Root fraction was increased for all sites except Brazil. Root growth rate was also increased for all sites. No soil parameters were modified.

SI3. Approach for normalization of yield and biomass data

We analyzed the relationship between mean growing season temperature and seed yield (and biomass) utilizing data from model simulations at temperature levels ranging from 0 to +9°C (Supplementary Fig. 1). We first normalized yield by year, location, model, and calibration. Given that mean growing season temperature under the 0ºC treatment varied from year to year, data were normalized to a common baseline temperature within a location, and not relative to the 0ºC treatment. We used the mean growing season temperature at each site during the experimental years of calibration at each location as the common baseline temperature to normalize data. To do this, absolute yield values were first fit to a quadratic model by site, year, model, and calibration, and the yield at the mean growing season temperature at each site by site, year, model, and calibration was obtained from this equation. Thereafter, absolute yield values across all temperature treatments within a site, year, model, and calibration were normalized dividing by the yield estimated from the quadratic model described above. We found that this quadratic model fit of absolute yield provided a good fit to our data (R^2>0.84 across all site, years, models and calibration combinations).

SI4. Literature review on previous temperature and [CO_2] studies

Experiments evaluating temperature effects

Limited literature exists on soybean yield response to elevated temperature under field conditions. We compared our results with temperature experiments conducted in out-door heated plots (Burkey et al., 2020; Ruiz-Vera et al., 2013), temperature gradient chambers (Baek et al., 2020; Tacarindua et al., 2013), and controlled environment growth chamebrs (Xu et al., 2016) (Fig. 6b). Burkey et al. (2020) planted soybean in out-door air exclusion system with double-wall panels on each side of the plot with fan boxes maintaining temperature around 3.4°C higher than the ambient of 25.65°C in Raleigh, North Carolina, US. Ruiz-Vera et al. (2013) grew soybean in the SoyFACE research facility in Champaign, Illinois, US, where plants were heated using out-door infrared lamps during the two years of experiment (2009 and 2011). Some of the studies conducted under temperature gradient chambers and controlled environment growth chambers pose limitations to compare absolute yield responses with those obtained in out-door heated plots and from model simulations. However, these were still informative to include in our literature review acknowledging this possible limitation and when expressing temperature effects on yield as a percentage change relative to baseline conditions. Tacarindua et al. (2013) grew soybean in temperature gradient chambers covered with polyethylene terephthalate film in Kyoto City, Japan, to increase temperature 1–3°C above the ambient of 25.7–27.1°C in the four years of experiment (2009–2012). Baek et al. (2020) also conducted experiments using temperature gradient chambers, which are plastic hoop greenhouses 2.5 m wide and 25 m long, warmed using ventilation fans and heaters to maintain temperature 1–4°C higher than the ambient (~24°C) at Wanju, Korea during one year (2019). Xu et al. (2016) conducted experiments in controlled environment growth chambers (EGC Corp., Chagrin Falls, OH, USA). In these experiment soybean was grown in pots and temperature was maintained at 6°C below or 8°C above the ambient temperature of 28/24°C (day/night). Alsajri et al. (2020) grew two soybean cultivars in soil-plant-atmosphere-research (SPAR) chambers in Starkville, MS, which are outdoor sunlit controlled environment chambers receiving almost normal diurnal solar radiation. They maintained day/night temperatures at five levels 21/13, 25/17, 29/21, 33/25, and 37/29°C. They reported seed yield reduction from the optimum temperature (25°C) to the highest temperature level (33°C). To compare results from these studies that evaluated different temperature increases from the baseline, we calculated the rate of yield change per 1°C increase in temperature in each study and from the ensemble model simulations. We limited studies and treatments included in our comparison to temperature increases above 1.5°C. This was to compare temperature responses close to the temperature increases simulated by models in our study, and to avoid an overestimation of the temperature effect when assuming a linear response to temperature.

Experiments evaluating [CO_2] effects

We compared our simulation results with those obtained experimentally after classifying in two groups based on the level of [CO_2] increase evaluated (range 540–600 ppm and 600–800 ppm, Fig. 8b). Some of the studies with evaluating elevated [CO_2] in soybean were conducted at FACE facilities in Illinois, USA (Bishop et al., 2015; Gray et al., 2016; Morgan et al., 2005; Ruiz-Vera et al., 2013), and Beijing, China (Hao et al., 2014). The SoyFACE facility in Champaign, Illinois is on natural field soil, where soybean and corn (Zea mays) are rotated annually on a tile drained field, and plots are fumigated to provide different elevated [CO_2] levels. Morgan et al.

(2005) reported results from the early experiments conducted in this facility during 2001-2003, with ambient and elevated [CO_2] levels of 370 and 550 ppm, respectively. Bishop et al. (2015) reported results from 2004-2008 across 18 genotypes, maintained at ambient (380-390 ppm) and elevated (547–552 ppm) [CO_2] levels. Ruiz-Vera et al. (2013) conducted experiments in 2009 and 2011 under ambient (385–390 ppm) and elevated (585–590) [CO_2] levels. Gray et al. (2016) presented results from 2004-2011 at ambient (376–392 ppm) and elevated (550-585 ppm) [CO_2] levels. In another FACE study conducted in Changping-Beijing, China (Hao et al., 2014), experiments were conducted in 2009 and 2011, and [CO_2] treatments included 415 and 550 ppm levels.

Apart from the field-grown FACE studies, we compared our results with studies conducted in naturally lit controlled environment growth chamber (Baker et al., 1989) and open-top chamber (Wang et al., 2018), and a meta-analysis of several studies (Ainsworth et al., 2002). In one of the early studies, Baker et al. (1989) grew soybean in naturally lit controlled environment growth chambers with cellulose acetate tops and mylar walls in year 1985, where [CO_2] were maintained at 330 and 660 ppm. Wang et al. (2018) carried out experiments in open-top chamber studies in Shanxi, China during 2013 and 2014, where [CO_2] was elevated to 200 ppm above the ambient level (~385 ppm). Xu et al. (2016) conducted experiments in controlled environment growth chambers (EGC Corp., Chagrin Falls, OH, USA) in 2014, where [CO_2] was maintained at two levels, 400 ppm and 800 ppm.

In the meta-analysis by Ainsworth et al. (2002), 111 studies published between 1980 to 2000 were included to extract elevated [CO_2] effect on various aspects of soybean growth, the elevated [CO_2] levels in the experiments ranged from 450−1250 ppm (elevated treatments), while the [CO_2] for baseline years can be considered between 340 to 370 ppm.

Supplementary Tables 1 to 9

Supplementary Table 1. Soybean crop models participating in the study and their approaches for modeling common crop growth and developmental processes.

Model	Leaf area development and light interception[a]	Photosynthesis method[b]	Yield partitioning[c]	Crop phenology[d]	Root distribution over depth[e]	Environmental factors affecting growth and yield partitioning[f]	Water stress approach[g]	Type of heat stress[h]	Soil water dynamics[i]	Evapotranspiration[j]	CO_2 effects[k]	Number of cultivar parameters	Number of reproductive growth stages
APSIM[1]	S	RUE	S/HI	T/DL/O	EXP	W/N/A/H	E/S	G	C	PT	RUE,TE	10	4
AQUACROP[2]	S	TE	HI	T/DL/O	EXP	W/ N/ H	E/S	P	C/R/O	P/ PM/PT	TE	7	2
DNDC[3]	S	TE-GC	HI	T/O	EXP	W/ N/H	S	P/B	C/O	PM	PT/TE	14	3
DSSAT[4]	I	P-R	S	T/DL/O	EXP	W/ N/H	E	P/Sn	C	PT	LF	18	5
DSSAT-EBL[5]	I	P-R	S	T/DL/O	EXP	W/N/H	E	P/Sn	C	EBL	LF	18	5
LINTUL[6]	D	RUE	Prt	T/DL	LIN	W/A/N/H	E	-	C	PM	RUE/TE	34	2
MONICA[7]	S	P-R	Prt	T/DL/O	EXP	W/N/A/H	E	P	C	PM	LF	32	3
SSM[8]	S	RUE	HI	T/DL/O	LIN	W/N/H	S	G	C	PT	RUE/TE	12	5
STICS[9]	S	RUE	HI/Prt	T/DL/O	SIG	W/N/H	E/S	G	C	PM	RUE	14	2
SWB[10]	S	Min(RUE/TE)	Prt	T/DL	EXP	W/N	S	-	C	PM	RUE/TE	27	3

[a]Leaf area development and light interception (S = Simple-unilayer; D = Detailed-multilayer approach; I = intermediate);

[b]Photosynthesis method (RUE = Radiation use efficiency approach, P-R = Gross photosynthesis–respiration, TE = Transpiration efficiency approach to compute biomass growth, TE-GC = Transpiration efficiency approach scaled by empirical biomass Growth Curve);

[c]Yield partitioning (HI = age-driven allocation coefficient or harvest index, S = Sink growth driven; Prt = partitioning during reproductive stages); Environmental factors affecting growth and yield partitioning (W = water stress on growth, N = nitrogen stress on growth, A = oxygen stress on growth, H = heat stress; P = photoperiod effect on sink growth or partitioning);

[d]Crop phenology (is a function of: T = temperature, DL = photoperiod (day length); O = other water/nutrient stress effects considered);

[e]Root distribution over depth (LIN = linear, EXP = exponential, SIG = sigmoidal, NON = no roots-just soil depth zone, CD = Convective Dispersive);

[f]Environmental factors affecting growth and yield partitioning (W = water stress on growth, N = nitrogen stress on growth, A = oxygen stress on growth, H = heat stress; P = photoperiod effect on sink growth or partitioning);

[g]Water stress approach (E = actual to potential evapotranspiration ratio; S = soil available water in root zone);

[h]Type of heat stress (G = quadratic growth/photosynthesis response to T; P= partitioning to yield; Sn=number of sinks); B = Beta distribution/plant growth response to T);

[i]Soil water dynamics (C = “Tipping bucket” capacity approach; R = Richards approach; O = others);

[j]Evapotranspiration (P = Penman; PM = Penman-Monteith; PT = Priestley-Taylor; EBL = Energy balance);

Soil C-N model (CN = CN model; N = N model; P(x) = x number of organic matter pools; B = microbial biomass pool);

[k]CO_2 approach (LF = Leaf-level photosynthesis-rubisco or on QE and Amax; RUE = Radiation use efficiency, TE = Transpiration efficiency, PT = Photosynthesis).

Model references: [1](Holzworth et al., 2014), [2](Steduto et al., 2009), [3](Smith et al., 2020), [4] (Boote et al., 1998; Hoogenboom et al., 2019), [5](Cuadra et al., 2020), [6](Kuhn et al., 2020), [7](Nendel et al., 2011b), [8](Sinclair, 1986; Soltani et al., 2012), [9](Brisson et al., 2003; Brisson et al., 2009), [10](Annandale et al., 2000; van der Laan et al., 2010)

Supplementary Table 2a. Temperature response functions for plant processes in models used in our study. Shaded cells indicate the model does not account for this process or temperature effects on it. Numbers in brackets indicate the cardinal temperatures in ºC describing temperature functions [e.g. (T1, T2, T3, T4) indicates a base temperature of T1, optimal temperatures between T2 and T3, and an upper failure temperature of T4].

Model	**Phenology**			**Growth and leaf/canopy expansion**			
	Vegetative phase /rate of leaf appearance	**Early reproductive phase**	**Late reproductive phase**	**Radiation Use Efficiency**	**Leaf photosynthesis**	**Leaf expansion**	**Internode length**
APSIM	L-Ta(10, 30, 30 40)	L-Ta(10, 30, 30, 40)	L-Ta(10, 30, 30, 40)	L-Ta(10, 20, 30, 40)			
AQUACROP	L-Ta(5,30, ∞,∞)	L-Ta(5,30, ∞,∞)	L-Ta(5,30, ∞,∞)				
DNDC	B-Ta(5,29,29,40)	B-Ta(5, 29, 29,40)	B-Ta(5, 29, 29,40)				
DSSAT	L-Ta(7, 28, 35, 45)	L-Ta(6, 26, 30, 45)	L-Ta(-15, 26, 34, 45)		L-Ta(0,8,40, 44,48,55)[1] Q-Tm(0,19,50,60)[2]	L-Ta(8,22, ∞, ∞)[3]	L-Ta(4,26, ∞, ∞)
LINTUL	L-Ta(7, 22, 30, 45)	L-Ta(7, 22, 30, 45)	L-Ta(7, 22, 30, 45)	Ta-(8,15,35,50)			
MONICA	L-Ta(8,30, ∞,∞)[3]	L-Ta(6,25, ∞,∞)[3]	L-Ta(-15,25, ∞,∞)[3]		L-Ta(5,25, 36,40)1		
SSM	L-Ta(7, 27, 34 ,45)	L-Ta(7, 27, 34 ,45)	L-Ta(7, 27, 34 ,45)	L-Ta(10, 20, 30, 40)			
STICS	L-Ta(5,25,25,45)	L-Ta(5,25,25,45)	L-Ta(5,25,25,45)	Q-Tc(5,28,32,45)		L-Tc(4,25,25,45)	
SWB	L-Ta(10, 25, 25, ∞)	L-Ta(10, 25, 25, ∞)	L-Ta(10, 25, 25, ∞)	L-Ta(10, 25, 25, ∞)			

L = linear look up function; Q = Quadratic/parabolic look up function; B = Beta distribution.
Ta, mean daily air temperature; Tx, daily maximum air temperature; Tm, daily minimum air temperature; Th, hourly or sub daily air temperature; Tc, canopy temperature; Txc, daily maximum canopy temperature; Tmc, daily minimum canopy temperature; Thc, sub daily canopy temperature; Ts, soil temperature; TT, thermal time;
[1] Temperature effect on leaf photosynthesis through effect on light saturated electron transport rate.
[2] Temperature effect on leaf photosynthesis through effect of minimum temperature from previous day on light-saturated leaf photosynthesis rate.
[3] Temperature effect on specific leaf area.

Supplementary Table 2b. (continuation) Temperature response functions for plant processes in models used in our study. Shaded cells indicate the model does not account for this process or temperature effects on it. Letters before the dash indicate the shape of the temperature response, and letters after the dash indicate the type of temperature inputs used. Numbers in brackets indicate the cardinal temperatures in ºC describing temperature functions [e.g. (T1, T2, T3, T4) indicates a base temperature of T1, optimal temperatures between T2 and T3, and an upper failure temperature of T4]

Model		**Reproductive growth**			**Biological nitrogen fixation**	
	Maintenance respiration	**Harvest index**	**Pod addition**	**Seed growth**	**N fixation**	**Nodule growth**
APSIM						
AQUACROP						
DNDC		Reduction based on heat stress above 29°C during anthesis		B-Ta(5, 29, 29, 40)		
DSSAT	Q_{10}-Ta[1]		Q-Ta(14, 21, 26.5, 40)	Q-Ta(6, 21, 23.5, 41)	L-Ta(5, 20, 35, 44)	L-Ta(7, 22, 35, 44)
LINTUL						
MONICA						
SSM						
STICS		Tmc=5 Txc=30 and no filling below and above			L-Ts (5,25,30,40)	L-Ta(5,25,25,45)
SWB						

L = linear look up function; Q = Quadratic/parabolic look up function; Q_{10}=coefficient of fractional change in process rate per 10 ºC increase in temperature; ; B = Beta distribution.
Ta, mean daily air temperature; Tx, daily maximum air temperature; Tm, daily minimum air temperature; Th, hourly or sub daily air temperature; Tc, canopy temperature; Txc, daily maximum canopy temperature; Tmc, daily minimum canopy temperature; Thc, sub daily canopy temperature; Ts, soil temperature; TT, thermal time;
[1]Maintenance respiration is a function of total biomass at 3.5*10-4 g CH_2O g^{-1} dry mass $hour^{-1}$, and of daily gross photosynthesis at 0.004 g CH_2O g^{-1} CH_2O from photosynthesis $hour^{-1}$, and these rates increase by a ratio of 1.9 per 10ºC increase in temperature above 20ºC.

Supplementary Table 3. Field experiment locations, growing season weather conditions, and summary of treatments used for the simulation exercise in this study.

Site	ARGN	FRNC	IOWA	BRZL	AKNS
Location	Azul (Argentina)	Auzeville (France)	Ames, IA (US)	Brasilia (Brazil)	Fayetteville, AR (US)
Latitude	−36.45	43.52	42.017	−15.59	36.01
Longitude	−59.50	1.51	−93.75	−47.74	−94.18
Elevation (m)	132	142	329	1007	432
[a]Precipitation, mm	519	253	576	640	265
[a]Temperature, ºC	19.8	21.2	21.7	22.7	25.0
[a]Solar radiation, MJ m^{-2} d^{-1}	24.2	20.9	20.2	18.7	20.1
Number of treatments	6	4	4	2	3
Treatments	three years, two water levels	two years, two water levels	two years, two planting dates	one year, two planting dates	three years
Experiment years	1999, 2000 & 2002	2017 & 2018	2015 & 2016	2017	2012, 2013, & 2014
Irrigation	Irrigated & rainfed	Irrigated & rainfed	Rainfed	Rainfed	Irrigated
Cultivar name	Don Mario	ISIDOR	Pioneer 92Y75R	BRS5980	42-M1
Cultivar MG	4	1	2	6	4
[b]Soil type	Loam	Clay loam	Clay loam	Clay	Silt loam
[c]Soil water LL	0.14	0.19	0.19	0.14	0.11
[c]Soil water DUL	0.30	0.34	0.33	0.28	0.27
Soil depth (m)	1.80	1.50	2.10	1.50	0.80
Data source	Adriana Confalone	Philippe Debaeke	Sotirios V. Archontoulis	Fernando A. Macena da Silva	Larry C. Purcell

[a]Environmental conditions averaged across the crop-growing season from planting to harvest.
[b]Classification of the top 30 cm soil profile based on USDA soil textural triangle.
[c]Soil water lower limit (LL) and drained upper limit (DUL) on volumetric basis (m^3 m^{-3}).

Supplementary Table 4. Description of soil profiles in the five locations used in this study.

Location	Soil layer bottom depth (cm)	Clay (%)	Silt (%)	Bulk density (g cm^{-3})	Saturated hydraulic conductivity (cm h^{-1})	Soil water lower limit (mm^3 mm^{-3})	Soil water drained upper limit (mm^3 mm^{-3})	Soil water saturation (mm^3 mm^{-3})	Root growth factor (fraction)
ARGN	5	23	36	1.11	1.32	0.14	0.30	0.41	1.00
	15	23	36	1.12	1.32	0.14	0.30	0.41	1.00
	30	22	34	1.42	1.32	0.14	0.29	0.39	0.80
	45	24	36	1.50	1.32	0.14	0.31	0.42	0.75
	60	33	29	1.29	0.23	0.17	0.38	0.49	0.40
	90	33	29	1.30	0.23	0.17	0.37	0.49	0.40
	120	20	31	1.35	1.32	0.13	0.24	0.35	0.20
	150	20	31	1.35	1.32	0.13	0.24	0.35	0.20
	180	14	33	1.47	2.59	0.12	0.17	0.27	0.00
AKNS	10	10	54	1.16	0.68	0.11	0.27	0.49	1.00
	20	14	55	1.19	0.68	0.11	0.27	0.46	0.84
	40	26	51	1.24	0.68	0.14	0.28	0.42	0.47
	60	32	46	1.30	0.23	0.16	0.29	0.40	0.35
	80	31	43	1.34	0.23	0.15	0.27	0.39	0.15
BRZL	10	67	6	1.15	7.00	0.14	0.30	0.36	1.00
	20	67	6	1.12	7.00	0.14	0.28	0.34	1.00
	30	67	6	1.12	7.00	0.14	0.28	0.33	1.00
	40	67	6	1.12	7.00	0.14	0.28	0.33	0.42
	50	69	7	1.12	7.00	0.15	0.26	0.32	0.34
	60	69	7	1.12	7.00	0.15	0.26	0.32	0.22
	90	69	7	1.12	7.00	0.15	0.26	0.32	0.17
	120	70	6	1.12	7.00	0.18	0.26	0.32	0.16
	150	70	6	1.12	7.00	0.18	0.26	0.32	0.04
FRNC (2017)	30	30	32	1.45	0.23	0.18	0.38	0.42	1.00
	60	26	34	1.50	1.23	0.18	0.38	0.41	0.41
	90	34	37	1.55	0.23	0.18	0.38	0.39	0.22
	120	33	37	1.55	0.23	0.18	0.38	0.39	0.12
	150	33	37	1.55	0.23	0.18	0.38	0.39	0.04
FRNC (2018)	30	33	32	1.45	0.23	0.19	0.34	0.43	1.00
	60	32	32	1.50	0.23	0.19	0.34	0.41	0.41
	90	34	30	1.55	0.23	0.19	0.34	0.39	0.22
	110	34	30	1.55	0.23	0.19	0.34	0.41	0.14
	150	34	30	1.55	0.23	0.19	0.34	0.39	0.05
IOWA	10	29	30	1.35	0.62	0.19	0.33	0.47	1.00
	20	27	33	1.34	0.75	0.19	0.32	0.47	1.00
	40	29	33	1.38	0.52	0.19	0.33	0.46	0.55
	60	28	28	1.49	0.42	0.17	0.30	0.42	0.37
	120	22	29	1.56	0.69	0.14	0.25	0.39	0.17
	150	15	36	1.60	1.62	0.09	0.20	0.39	0.07
	180	15	36	1.60	0.23	0.09	0.20	0.29	0.04
	210	15	36	1.60	0.14	0.09	0.20	0.27	0.02

Supplementary Table 5. Analysis of variance table of the percent yield change when increasing [CO_2] from 360 ppm to 540 ppm, and when increasing temperature from the baseline by 3°C. Crop model, calibration, location, and their interactions were considered as fixed factors. Year nested within location, and the interaction of crop model and year nested within location were included as random factors in the model.

Source	Degrees of freedom	+3°C temperature increase			360 to 540 ppm [CO_2] increase		
		P > F	LW[¥]	% Sum of squares	P > F	LW	% Sum of squares
Model	10	<.0001	125.0	16.0	<.0001	>1000	58.9
Location	4	<.0001	17.7	10.0	<.0001	52.2	6.1
Calibration	1	<.0001	41.6	1.0	<.0001	35.1	0.5
Model*Location	39	<.0001	106.9	16.3	<.0001	303.3	15.1
Model* Calibration	10	<.0001	102.6	3.0	<.0001	153.3	2.9
Location* Calibration	4	<.0001	15.0	0.4	<.0001	31.5	0.5
Model*Location*Calibration	39	<.0001	96.0	3.4	<.0001	101.9	2.2
Year(Location)	148	<.0001	43.1	12.6	<.0001	7.5	1.5
Model*Year(Location)	1421	<.0001	162.4	29.7	<.0001	27.2	7.6
Residual	1569	.		7.7	.		4.8

[¥]LW or Logworth was calculated as –log10(p- value). Greater LW values indicate greater portion of the variability comes from that particular source, (LW=1.3 when P=0.05; LW =2 when P=0.01; LW =3 when P=0.001).

Supplementary Table 6. Mean percentage yield change from 30-yr simulations under a +3°C temperature increase from baseline conditions after *Blind* and *Full* calibration for each model, probability of the calibration effect within a location and model expressed as the LogWorth (LW).

Model	Yield change (%)														
	Argentina			France			Iowa			Brazil			Arkansas		
	Blind	*Full*	LW[¥]	*Blind*	*Full*	*LW*	*Blind*	*Full*	*LW*	*Blind*	*Full*	*LW*	*Blind*	*Full*	*LW*
APSIM	-9	29	101.5	-23	-10	13.3	-20	-16	1.8	-42	-38	1.5	-16	-16	0.0
AQUACROP	-18	-11	6.5	7	-4	9.0	-13	-14	0.1	-11	-16	2.4	-9	-11	0.5
DNDC	-8	-8	0.1	-4	-4	0.0	-7	-7	0.2	0	-1	0.0	-13	-13	0.0
DSSAT	9	8	0.3	0	0	0.2	2	0	0.7	-13	-12	0.1	-4	-3	0.1
DSSATEBL	14	8	3.6	4	0	2.2	0	2	0.3	-13	-13	0.1	-5	3	6.2
LINTUL	3	3	0.1	-16	-19	0.8	-7	-7	0.0	-13	-13	0.0	-11	-10	0.8
MONICA	-12	-16	1.8	-15	-14	0.4	-15	-21	3.2	-30	-35	2.6	-30	-32	0.6
SSM	2	17	16.8	-9	1	7.9	2	12	7.4	-23	3	47.0	-5	-2	1.3
STICS	-26	-2	41.5	-22	-1	29.8	-11	-8	1.0	-34	-25	7.0	-1	1	0.7
SWB[§]	-23	-24	3.9	.	.	.	1	3	0.3	-17	-10	3.7	-25	-20	3.7
Ensemble	-8	0	4.8	-11	-7	1.5	-7	-6	0.3	-21	-16	2.1	-13	-12	0.5

[¥] LW is calculated as –log10(p- value) from the probability of the effect of calibration obtained from the ANOVA of the % yield change (Supplementary Table 5). Greater LW values indicate a relatively lower probability of rejecting that the calibration effect is significant when comparing among models (LW=1.3 when P=0.05; LW =2 when P=0.01; LW =3 when P=0.001).

[§] France baseline has zero yield for many years, and temperature and [CO_2] response of yield did not follow the expected trend. It was thus removed from the analysis.

Supplementary Table 7. Mean percentage yield change from 30-yr simulations under a [CO_2] increase from 360ppm to 540 ppm after *Blind* and *Full* calibration for each model, probability of the calibration effect within a location and model expressed as the logworth (LW).

Model	Yield change (%)														
	Argentina			France			Iowa			Brazil			Arkansas		
	Blind	*Full*	LW[¥]	*Blind*	*Full*	*LW*	*Blind*	*Full*	*LW*	*Blind*	*Full*	*LW*	*Blind*	*Full*	*LW*
APSIM	17	14	3.1	17	17	0.3	20	18	3.1	26	21	12.3	19	19	0.0
AQUACROP	29	29	0.1	29	29	0.4	29	29	0.1	29	29	0.1	29	29	0.0
DNDC	28	26	2.4	15	14	0.3	13	12	0.3	24	24	0.0	15	15	0.0
DSSAT	19	18	1.6	19	18	0.3	19	19	0.2	22	20	2.9	24	24	0.3
DSSATEBL	26	18	37.0	24	18	20.2	19	21	2.0	23	20	3.5	18	16	2.9
LINTUL	25	26	0.6	22	22	0.1	28	30	2.0	40	41	0.6	32	34	9.2
MONICA	16	22	18.2	25	19	16.4	21	28	21.4	32	41	41.3	30	35	15.5
SSM	13	9	8.7	12	8	9.1	13	7	15.6	13	5	32.5	13	2	62.5
STICS	14	10	10.1	8	8	0.5	13	14	1.0	14	14	0.1	11	15	6.3
SWB[§]	21	14	28.7	.	.	.	17	15	2.4	21	13	33.3	17	19	3.7
Ensemble	20	18	1.6	19	17	2.7	19	19	0.2	24	21	4.3	21	21	0.5

[¥] LW is calculated as –log10(p- value) from the probability of the effect of calibration obtained from the ANOVA of the % yield change (Supplementary Table 5). Greater LW values indicate a relatively lower probability of rejecting that the calibration effect is significant when comparing among models (LW=1.3 when P=0.05; LW =2 when P=0.01; LW =3 when P=0.001)

[§] France baseline has zero yield for many years, and temperature and [CO_2] response of yield did not follow the expected trend. It was thus removed from the analysis.

Supplementary Table 8. Change in yield, biomass, and maximum LAI (%) under [CO_2] increase from 360 ppm to 540 or 720 ppm [CO_2], as simulated by the ensemble-mean of models after *Blind* and *Full* calibration.

	[CO_2] elevated to (ppm)	Yield change (%)		Biomass change (%)		Harvest index change (%)		LAI change (%)	
		Blind	*Full*	*Blind*	*Full*	*Blind*	*Full*	*Blind*	*Full*
ARGN	540	19.9	18.4	19.3	18.1	0.4	0.2	15.5	12.7
FRNC	540	18.8	16.8	17.4	16.9	1.1	-0.1	10.1	12.2
IOWA	540	19.0	19.4	17.9	19.6	1.0	-0.2	10.6	13.2
BRZL	540	23.6	20.9	22.9	21.8	0.6	-0.7	18.5	16.5
AKNS	540	20.8	21.5	20.5	23.1	0.2	-1.3	15.2	18.8
All sites	540	20.4	19.4	19.6	19.9	0.7	-0.4	14.0	14.7
ARGN	720	34.5	31.1	34.1	31.1	0.2	0.0	26.3	20.8
FRNC	720	32.0	28.3	30.0	28.9	1.6	-0.4	17.2	20.4
IOWA	720	32.8	33.1	31.1	33.9	1.3	-0.7	17.7	21.6
BRZL	720	40.6	35.8	39.7	38.5	0.6	-1.9	30.3	27.7
AKNS	720	36.0	37.1	35.9	40.2	0.0	-2.2	25.1	31.1
All sites	720	35.2	33.1	34.2	34.5	0.8	-1.0	23.3	24.3

Supplementary Table 9. Analysis of covariance table of the relative yield. Crop model, calibration, and location and their interaction were considered as fixed factors, average growing season temperature (T) and its square were covariates.

Source	Seed yield			Biomass		
	Degrees of freedom	Sum of Squares	P > F	Degrees of freedom	Sum of Squares	P > F
Calibration	1	19419	<.0001	1	0	0.922
Model	10	145402	<.0001	9	70602	<.0001
Model*Calibration	10	25959	<.0001	9	4594	<.0001
Location	4	63553	<.0001	4	27112	<.0001
Calibration*Location	4	1970	0.0001	4	3333	<.0001
Model*Location	39	192643	<.0001	35	93998	<.0001
Model*Calibration*Location	39	35617	<.0001	35	27610	<.0001
T	1	31993	<.0001	1	11674	<.0001
T*Calibration	1	19700	<.0001	1	21	0.45
T*Model	10	141019	<.0001	9	55384	<.0001
T*Model*Calibration	10	26833	<.0001	9	5244	<.0001
T*Location	4	60431	<.0001	4	27348	<.0001
T*Calibration*Location	4	2299	<.0001	4	3567	<.0001
T*Model*Location	39	220692	<.0001	35	109767	<.0001
T*Model*Calibration*Location	39	37864	<.0001	35	29429	<.0001
T*T	1	56729	<.0001	1	29827	<.0001
T*T*Calibration	1	3822	<.0001	1	265	0.007
T*T*Model	10	63346	<.0001	9	23107	<.0001
T*T*Location	4	17145	<.0001	4	13497	<.0001
T*T*Model*Calibration	9	11192	<.0001	9	2224	<.0001
T*T*Model*Location	24	35504	<.0001	22	38183	<.0001
T*T*Model*Calibration*Location	14	2457	0.0104	14	1728	<.0001
Residual	12519	1059282	.	11499	423408	.

Supplementary Figures 1 to 5

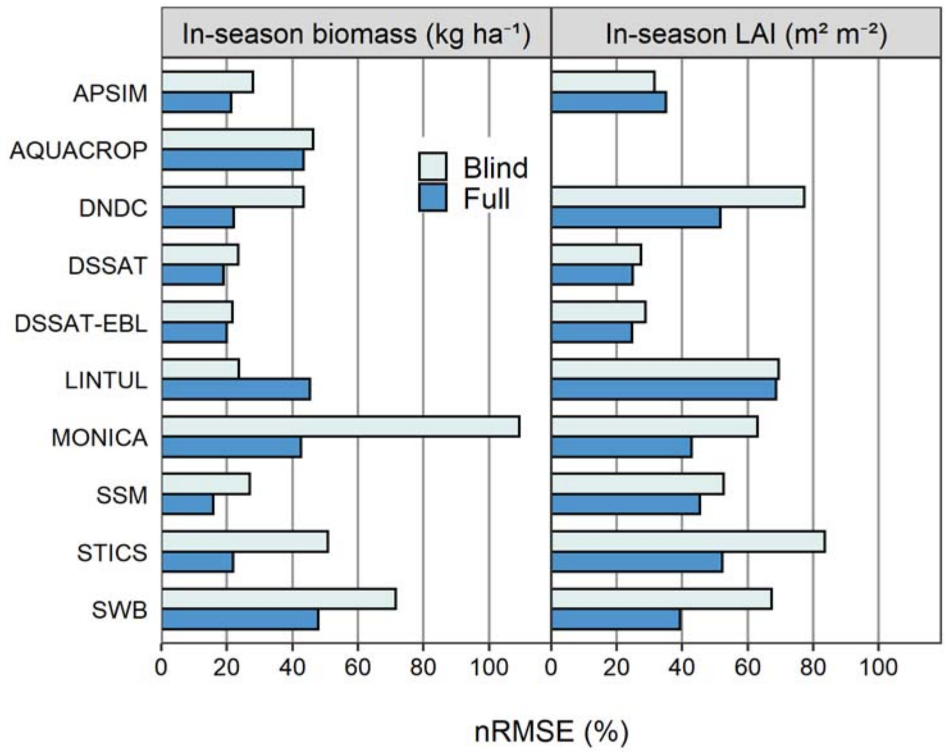

Supplementary Figure 1. Normalized root mean square error (nRMSE) for the simulation of in-season biomass and leaf area index (LAI) by individual models after *Blind* and *Full* calibration. The nRMSE was obtained for each model across treatments within a location, and then averaged across locations.

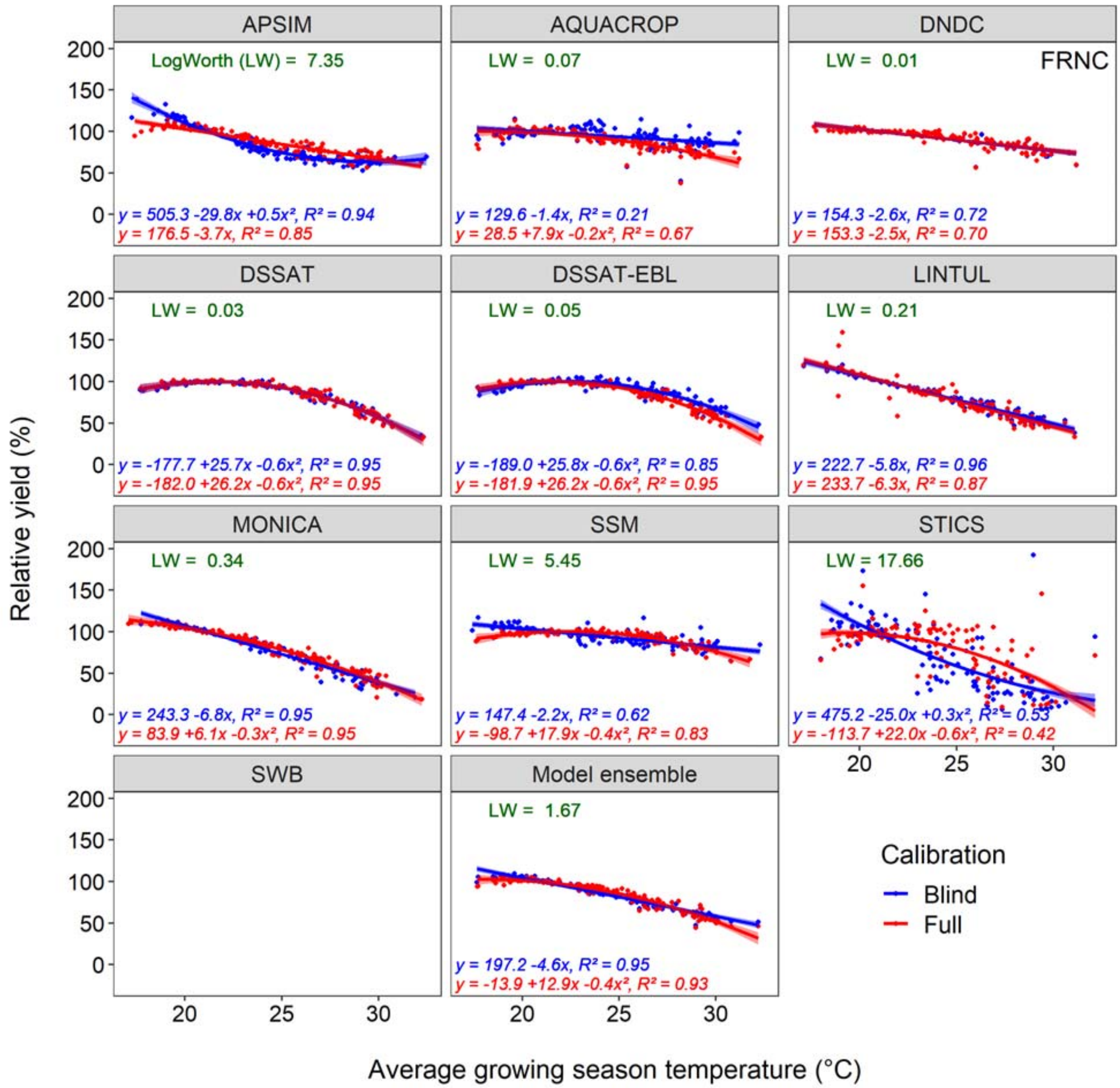

Supplementary Figure 2a. Relationship between relative yield and mean growing season temperature by model and calibration in France. Data from 30-year simulations and temperature treatments 0 to +9°C. The circles show simulated relative yield, while the lines are fitted quadratic or linear curves by model and calibration with equations and R^2 shown in figures. The bands are 90% confidence interval of the model fit. LogWorth values are the transformed probability values of the calibration effect within each model, with higher Logworth values indicating a lower probability that the calibration effect is not significant (e.g. LogWorth = 4 is equivalent to p=0.0001).

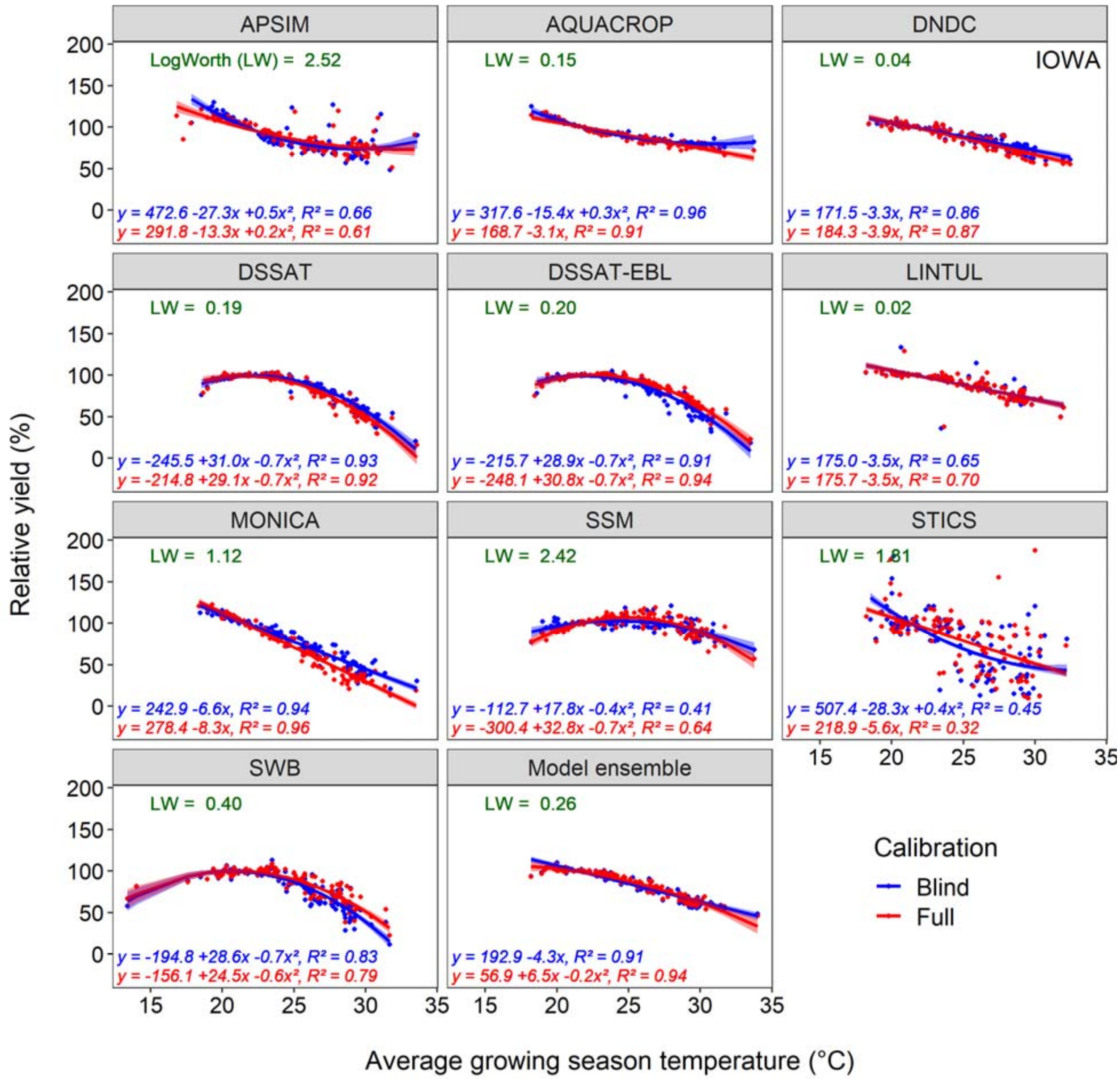

Supplementary Figure 2b. Relationship between relative yield and mean growing season temperature by model and calibration in Iowa. Data from 30-year simulations and temperature treatments 0 to +9°C. The circles show simulated relative yield, while the lines are fitted quadratic or linear curves by model and calibration with equations and R^2 shown in figures. The bands are 90% confidence interval of the model fit. LogWorth values are the transformed probability values of the calibration effect within each model, with higher Logworth values indicating a lower probability that the calibration effect is not significant (e.g. LogWorth = 4 is equivalent to p=0.0001).

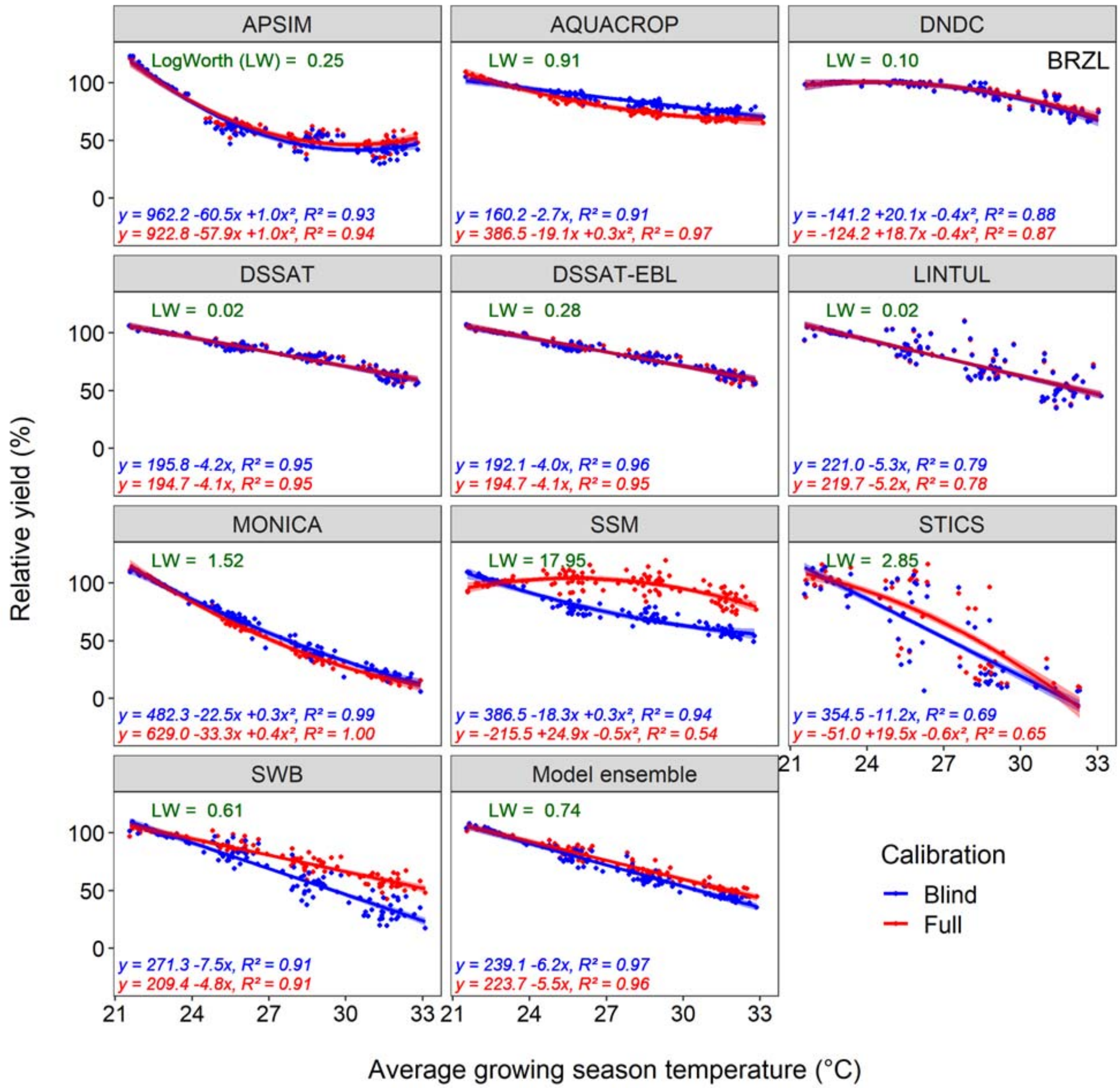

Supplementary Figure 2c. Relationship between relative yield and mean growing season temperature by model and calibration in Brazil. Data from 30-year simulations and temperature treatments 0 to +9°C. The circles show simulated relative yield, while the lines are fitted quadratic or linear curves by model and calibration with equations and R^2 shown in figures. The bands are 90% confidence interval of the model fit. LogWorth values are the transformed probability values of the calibration effect within each model, with higher Logworth values indicating a lower probability that the calibration effect is not significant (e.g. LogWorth = 4 is equivalent to p=0.0001).

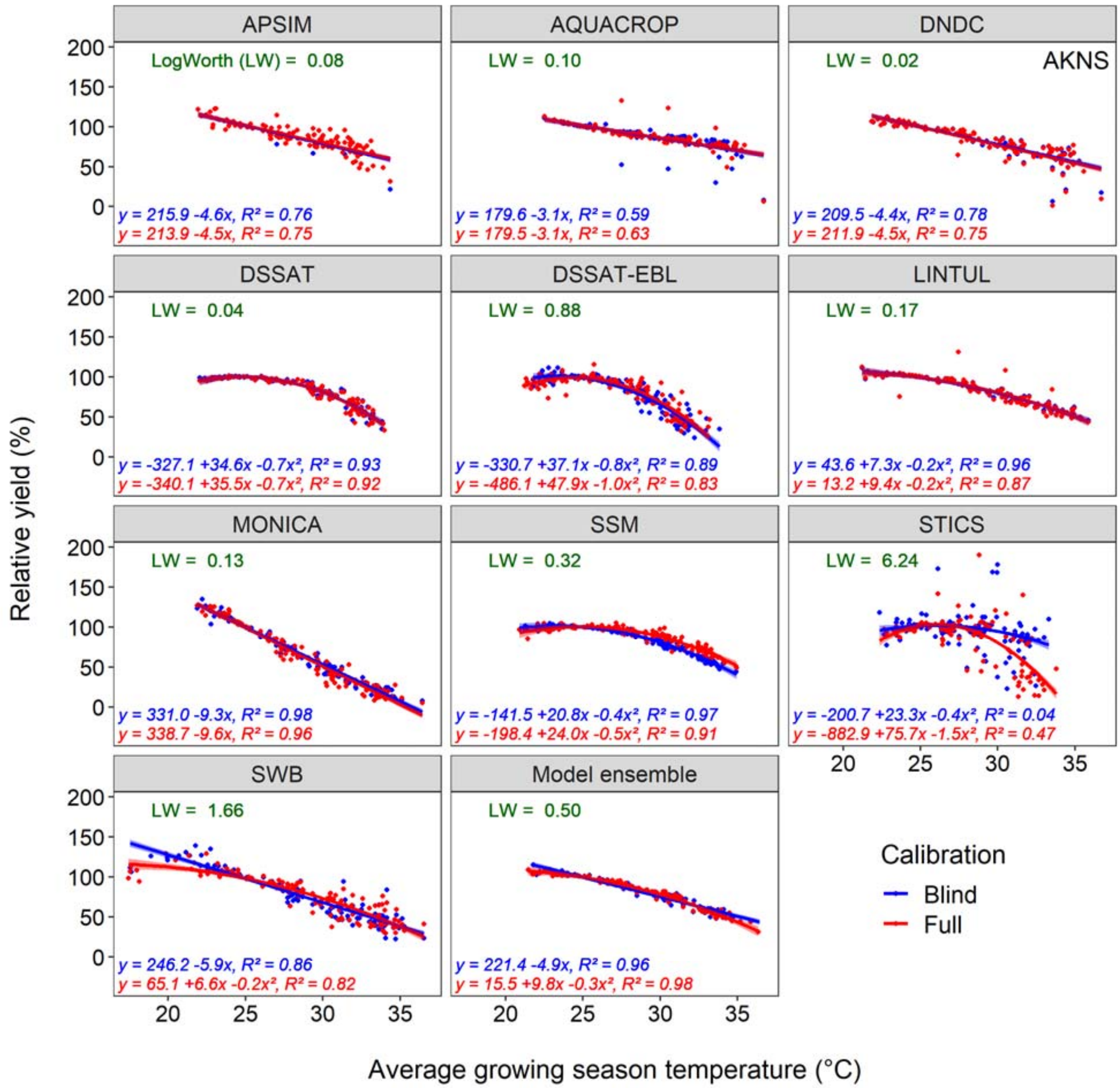

Supplementary Figure 2d. Relationship between relative yield and mean growing season temperature by model and calibration in Arkansas. Data from 30-year simulations and temperature treatments 0 to +9°C. The circles show simulated relative yield, while the lines are fitted quadratic or linear curves by model and calibration with equations and R^2 shown in figures. The bands are 90% confidence interval of the model fit. LogWorth values are the transformed probability values of the calibration effect within each model, with higher Logworth values indicating a lower probability that the calibration effect is not significant (e.g. LogWorth = 4 is equivalent to p=0.0001).

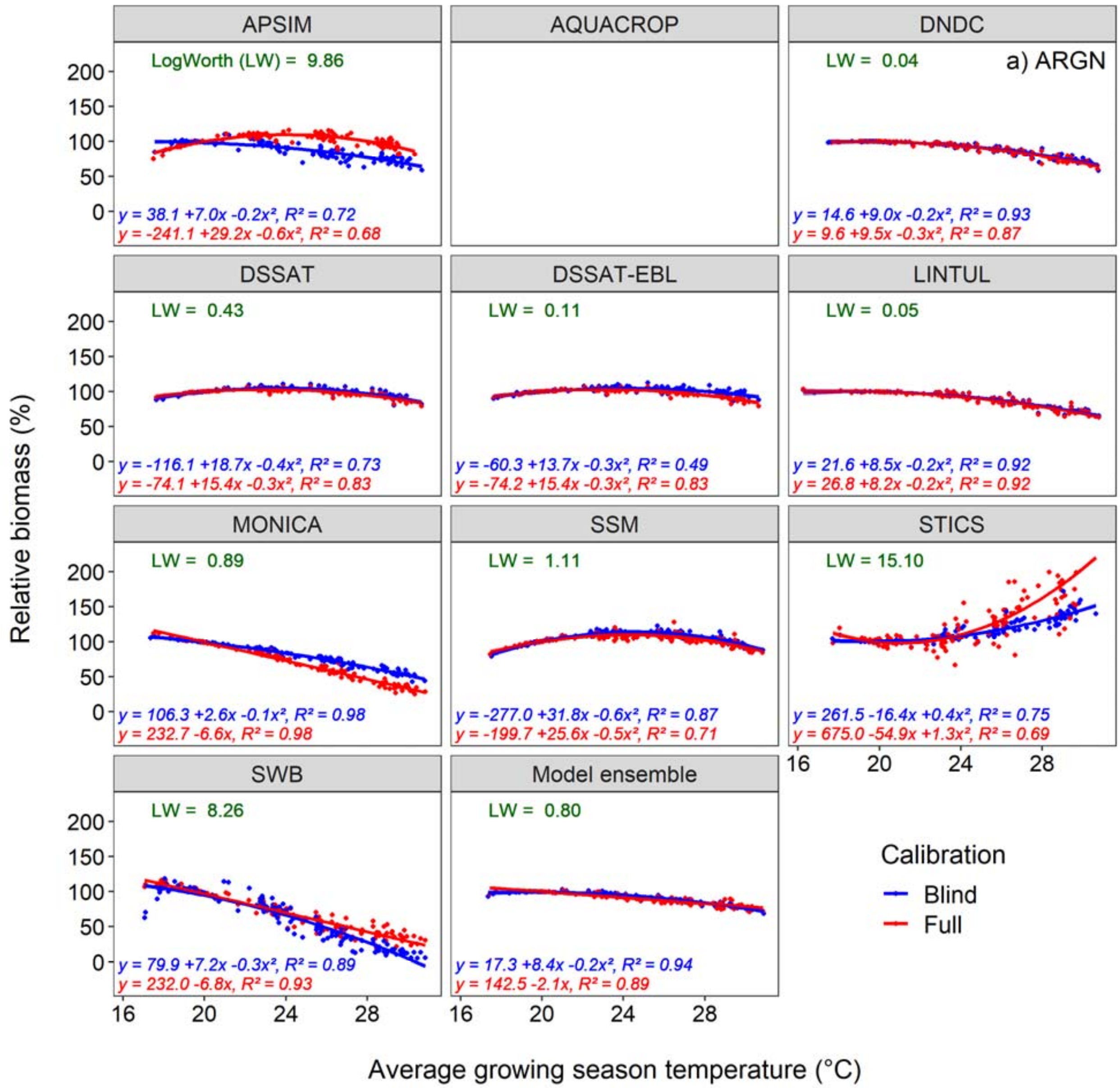

Supplementary Figure 3a. Relationship between relative biomass and mean growing season temperature by model and calibration in Argentina. Data from 30-year simulations and temperature treatments 0 to +9°C. The circles show simulated relative biomass, while the lines are fitted quadratic or linear curves by model and calibration with equations and R^2 shown in figures. The bands are 90% confidence interval of the model fit. LogWorth values are the transformed probability values of the calibration effect within each model, with higher Logworth values indicating a lower probability that the calibration effect is not significant (e.g. LogWorth = 4 is equivalent to p=0.0001).

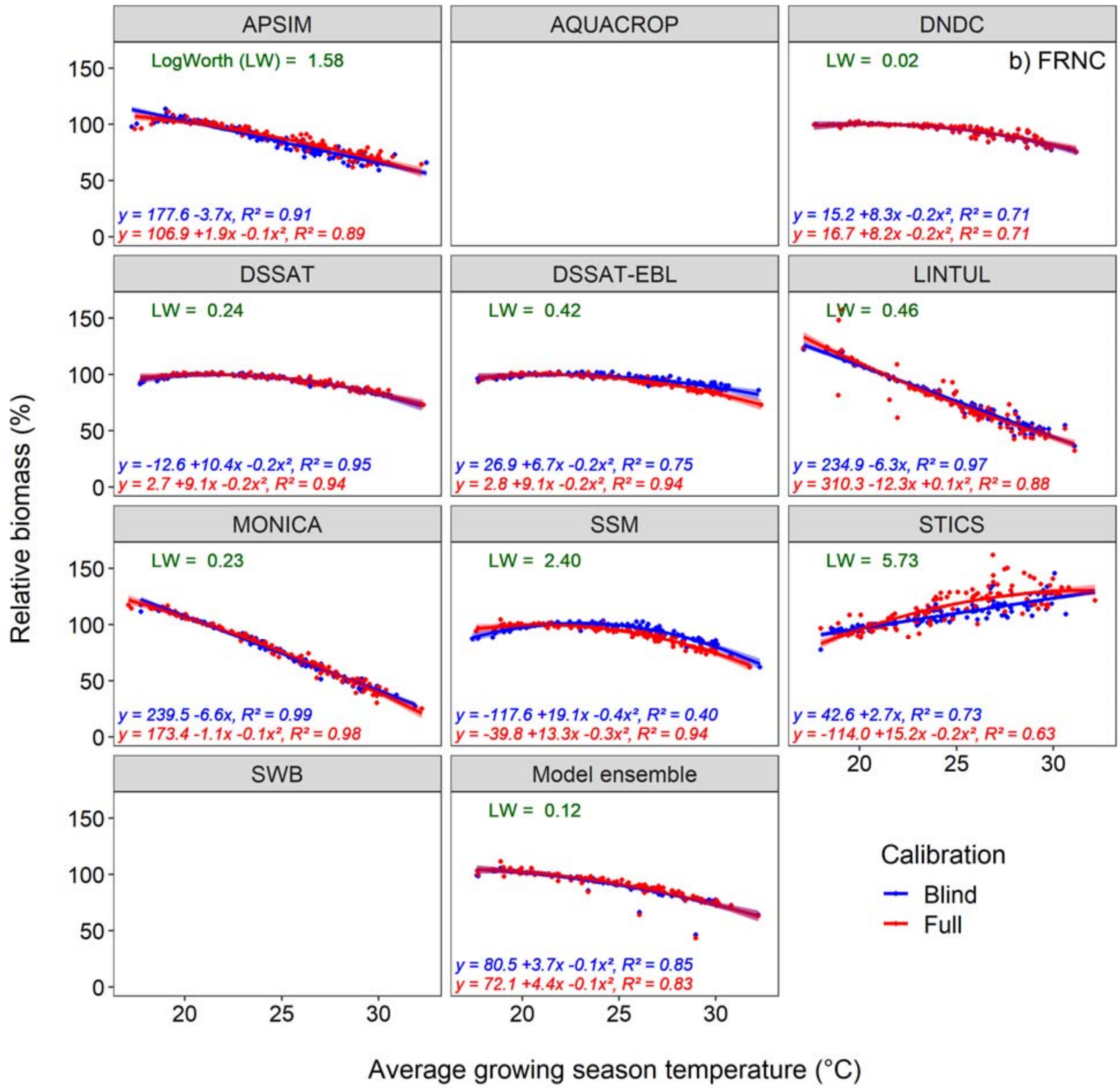

Supplementary Figure 3b. Relationship between relative biomass and mean growing season temperature by model and calibration in France. Data from 30-year simulations and temperature treatments 0 to +9°C. The circles show simulated relative biomass, while the lines are fitted quadratic or linear curves by model and calibration with equations and R^2 shown in figures. The bands are 90% confidence interval of the model fit. LogWorth values are the transformed probability values of the calibration effect within each model, with higher Logworth values indicating a lower probability that the calibration effect is not significant (e.g. LogWorth = 4 is equivalent to p=0.0001).

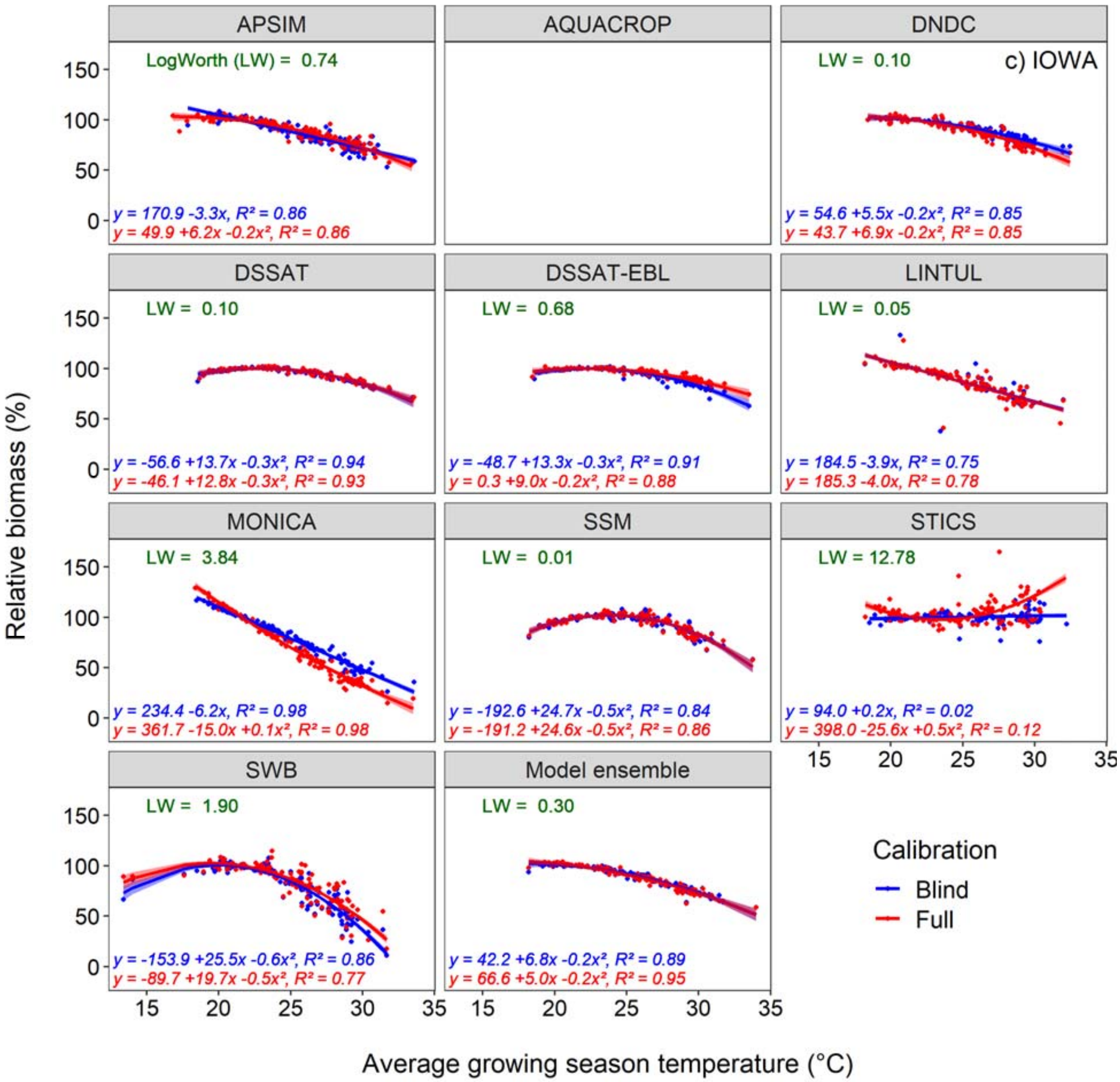

Supplementary Figure 3c. Relationship between relative biomass and mean growing season temperature by model and calibration in Iowa. Data from 30-year simulations and temperature treatments 0 to +9°C. The circles show simulated relative biomass, while the lines are fitted quadratic or linear curves by model and calibration with equations and R^2 shown in figures. The bands are 90% confidence interval of the model fit. LogWorth values are the transformed probability values of the calibration effect within each model, with higher Logworth values indicating a lower probability that the calibration effect is not significant (e.g. LogWorth = 4 is equivalent to p=0.0001).

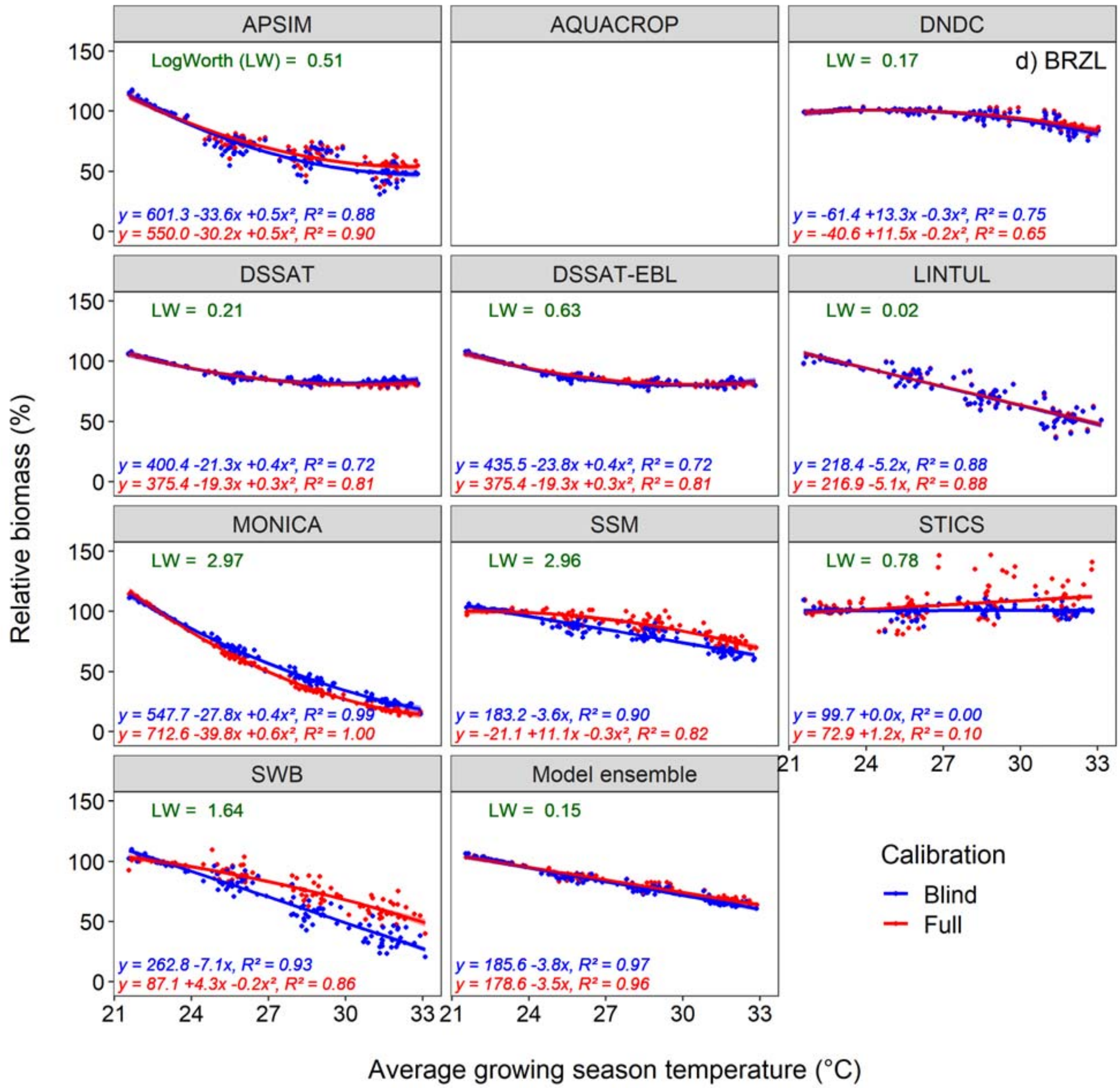

Supplementary Figure 3d. Relationship between relative biomass and mean growing season temperature by model and calibration in Brazil. Data from 30-year simulations and temperature treatments 0 to +9°C. The circles show simulated relative biomass, while the lines are fitted quadratic or linear curves by model and calibration with equations and R^2 shown in figures. The bands are 90% confidence interval of the model fit. LogWorth values are the transformed probability values of the calibration effect within each model, with higher Logworth values indicating a lower probability that the calibration effect is not significant (e.g. LogWorth = 4 is equivalent to p=0.0001).

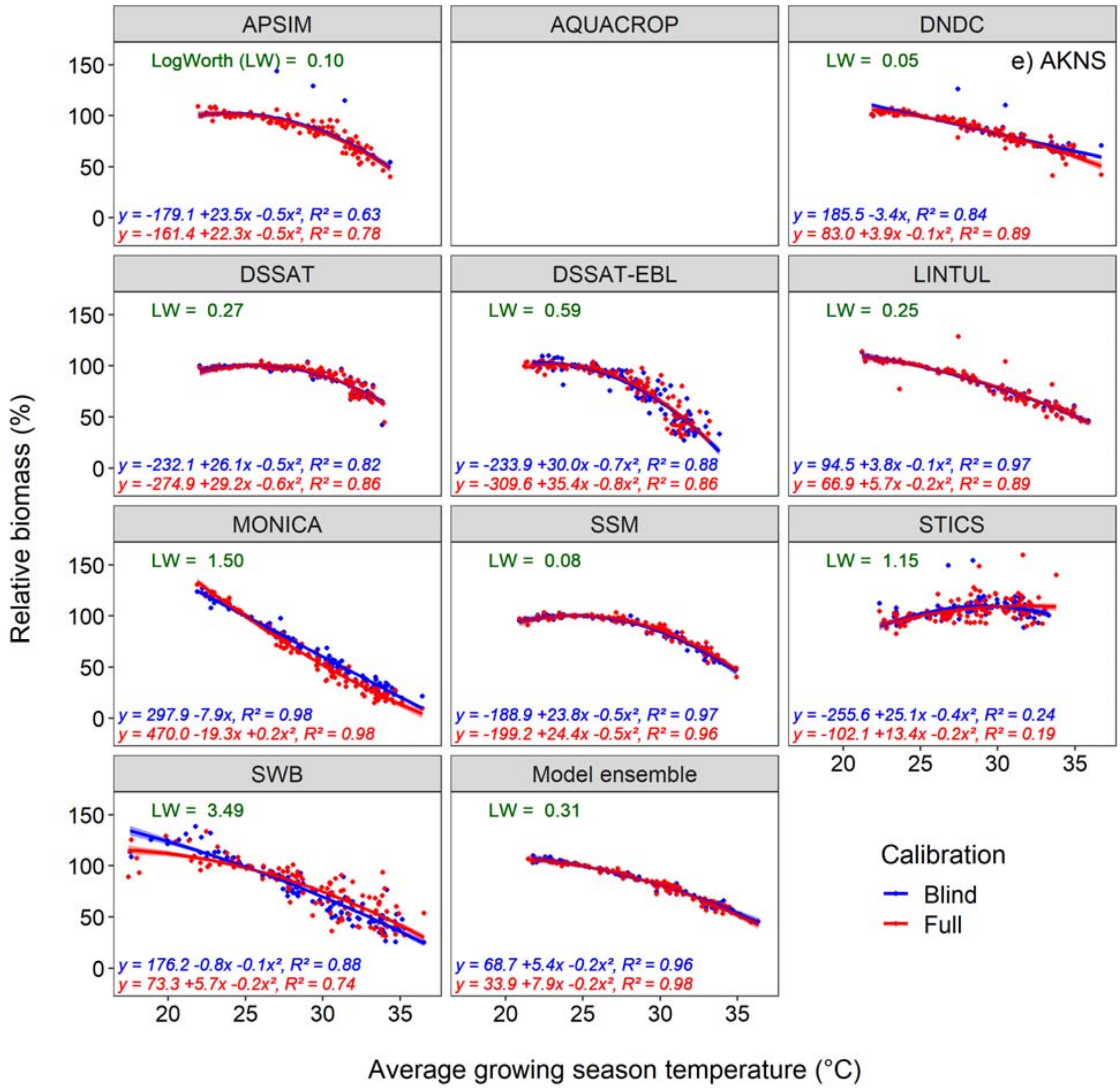

Supplementary Figure 3e. Relationship between relative biomass and mean growing season temperature by model and calibration in Arkansas. Data from 30-year simulations and temperature treatments 0 to +9°C. The circles show simulated relative biomass, while the lines are fitted quadratic or linear curves by model and calibration with equations and R^2 shown in figures. The bands are 90% confidence interval of the model fit. LogWorth values are the transformed probability values of the calibration effect within each model, with higher Logworth values indicating a lower probability that the calibration effect is not significant (e.g. LogWorth = 4 is equivalent to p=0.0001).

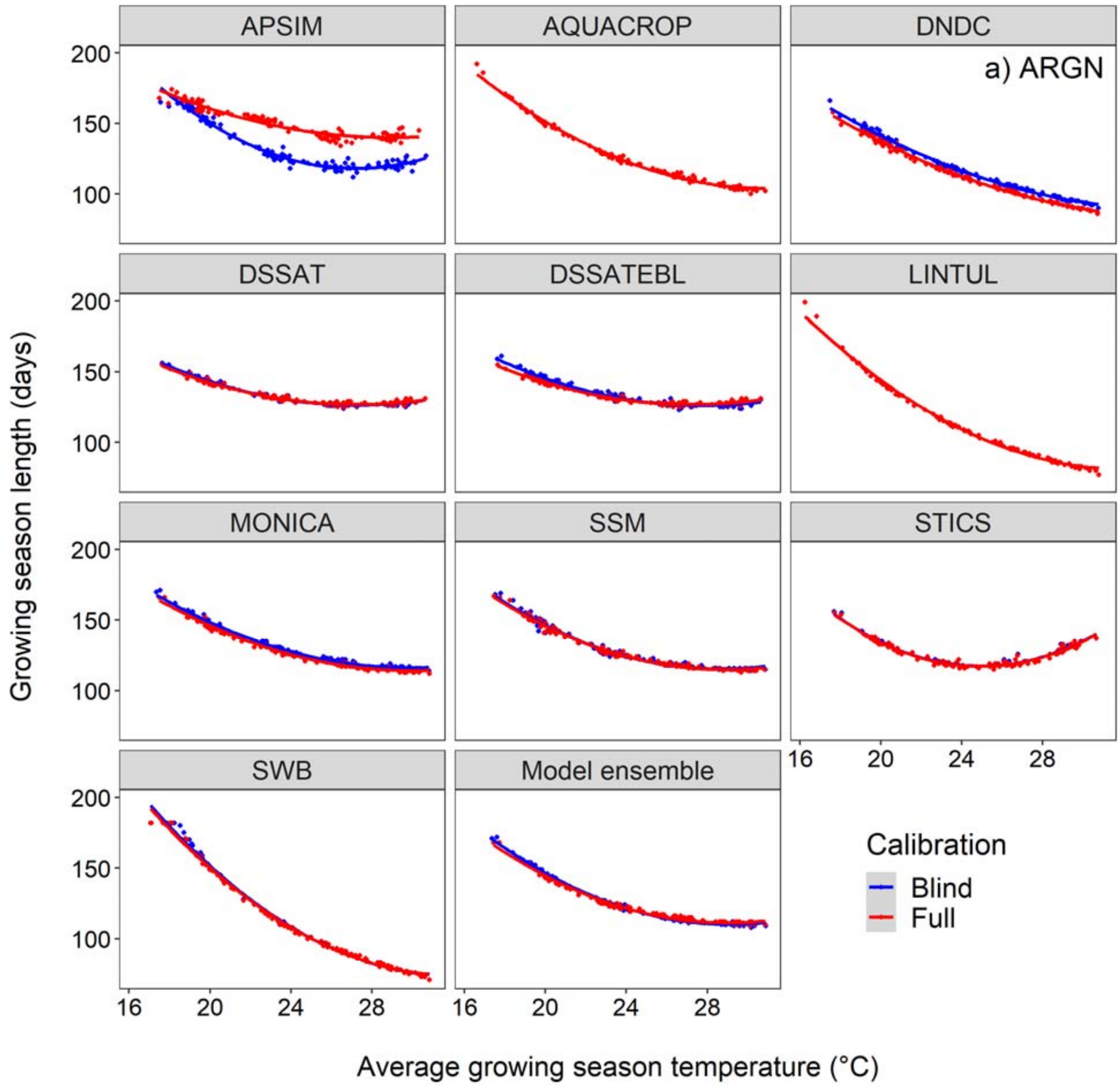

Supplementary Figure 4a. Relationship between simulated growing season length (days) and mean growing season temperature by model in **Argentina**. Data plotted from 30 year simulations and temperature modification of 0, +3, +6, and +9°C from the baseline. The circles show simulated values while the lines are quadratic curves fitted using the "stat_smooth" function and "lm" method in R version 4.0.2 using a quadratic model.

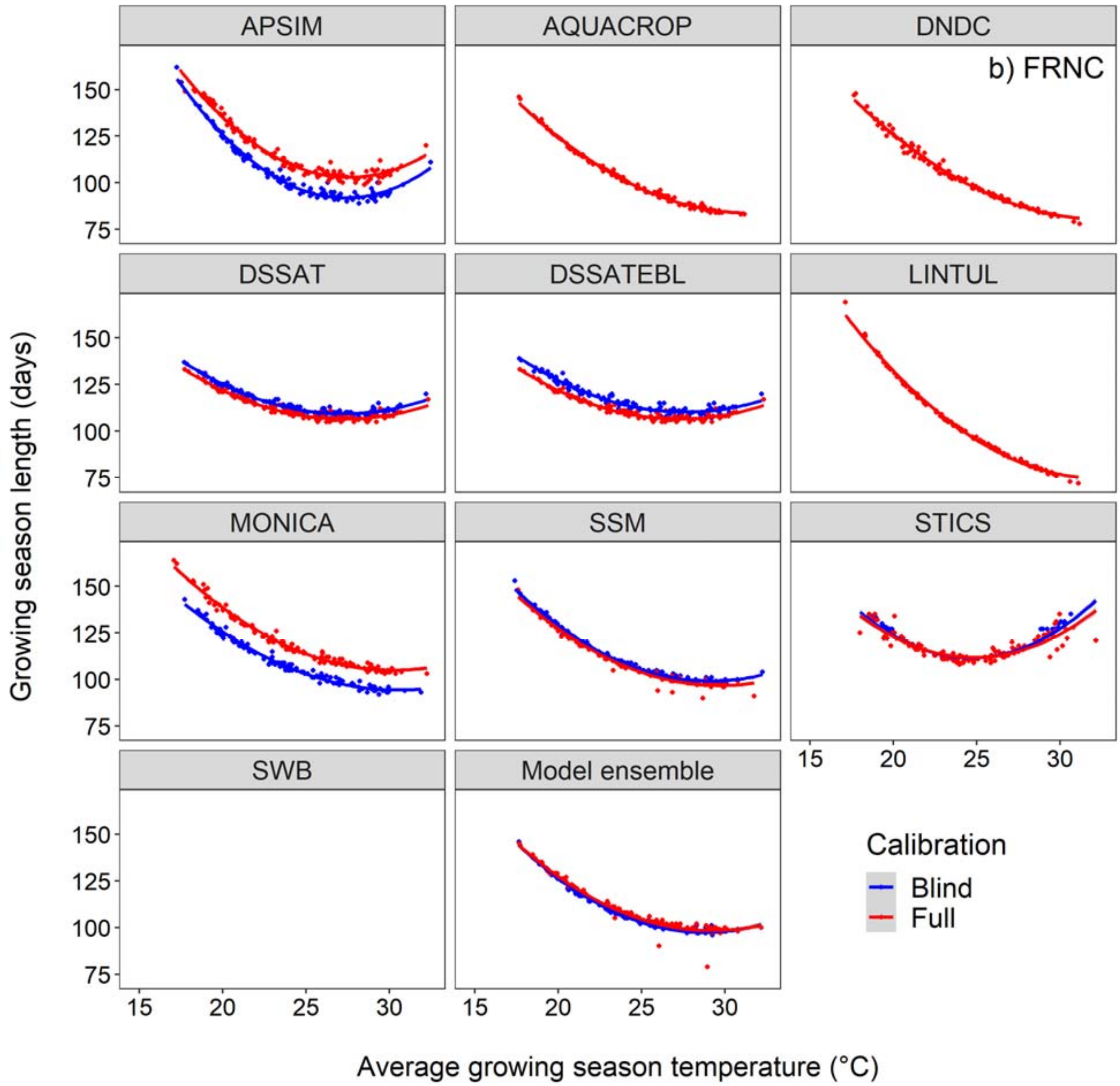

Supplementary Figure 4b. Relationship between simulated growing season length (days) and growing season temperature by model in **France**. Data plotted includes simulated yield across 30 years and temperature modification of 0, +3, +6, and +9°C from the baseline. The circles show simulated values while the lines are quadratic curves fitted using the "stat_smooth" function and "lm" method in R version 4.0.2 using a quadratic model.

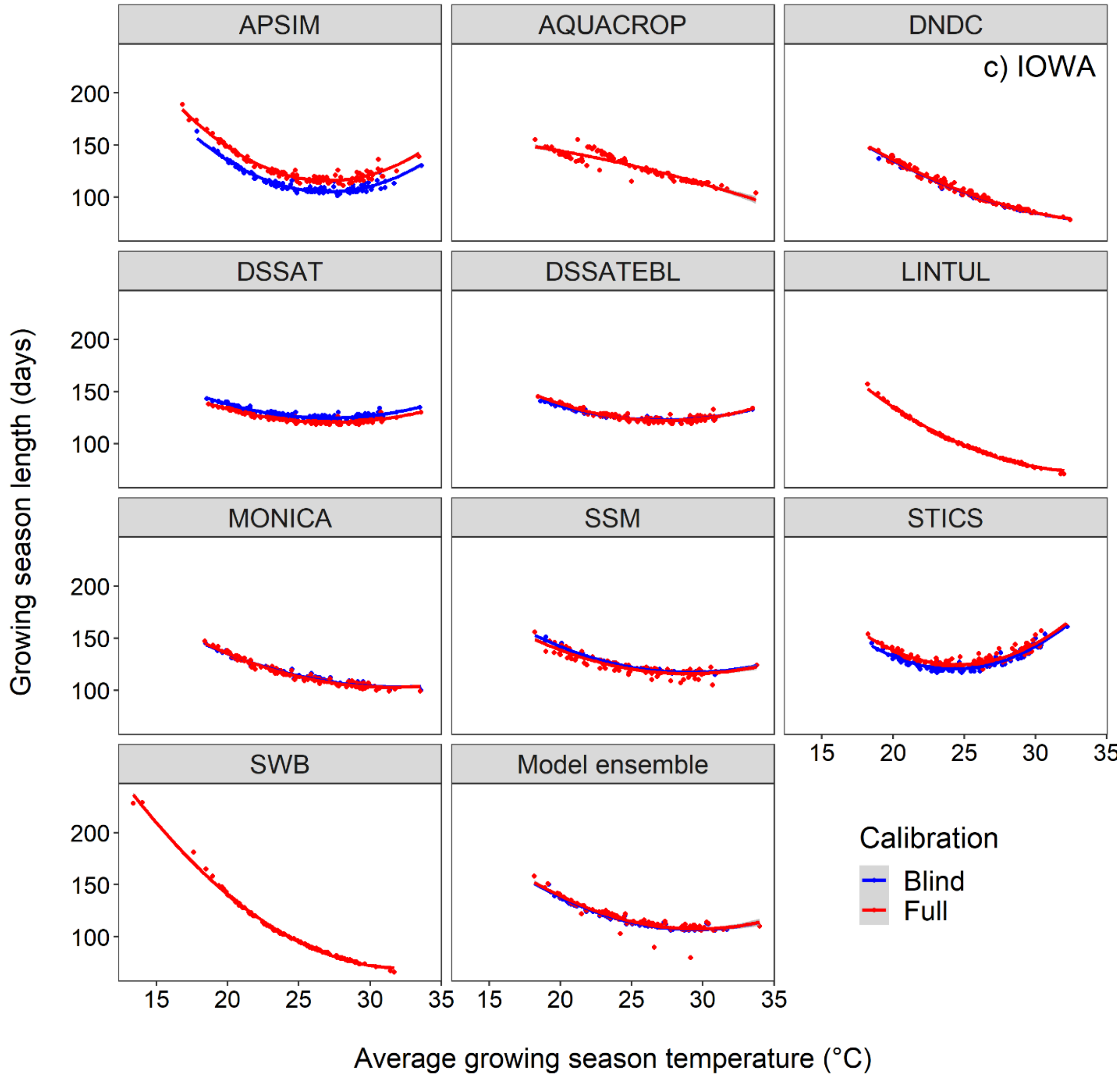

Supplementary Figure 4c. Relationship between simulated growing season length (days) and growing season temperature by model in **Iowa**. Data plotted includes simulated yield across 30 years and temperature modification of 0, +3, +6, and +9°C from the baseline. The circles show simulated values while the lines are quadratic curves fitted using the "stat_smooth" function and "lm" method in R version 4.0.2 using a quadratic model.

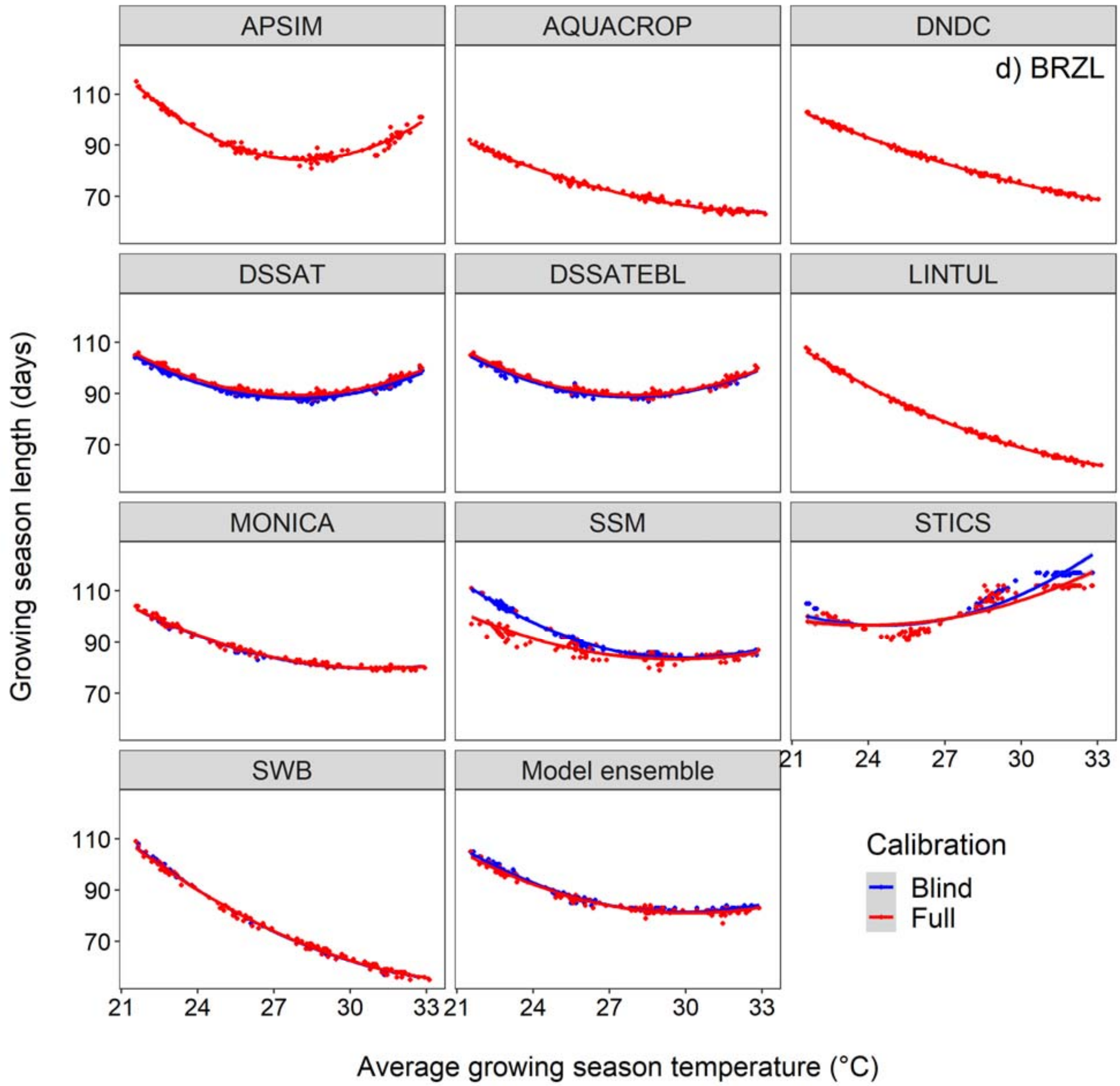

Supplementary Figure 4d. Relationship between simulated growing season length (days) and growing season temperature by model in **Brazil**. Data plotted includes simulated yield across 30 years and temperature modification of 0, +3, +6, and +9°C from the baseline. The circles show simulated values while the lines are quadratic curves fitted using the "stat_smooth" function and "lm" method in R version 4.0.2 using a quadratic model.

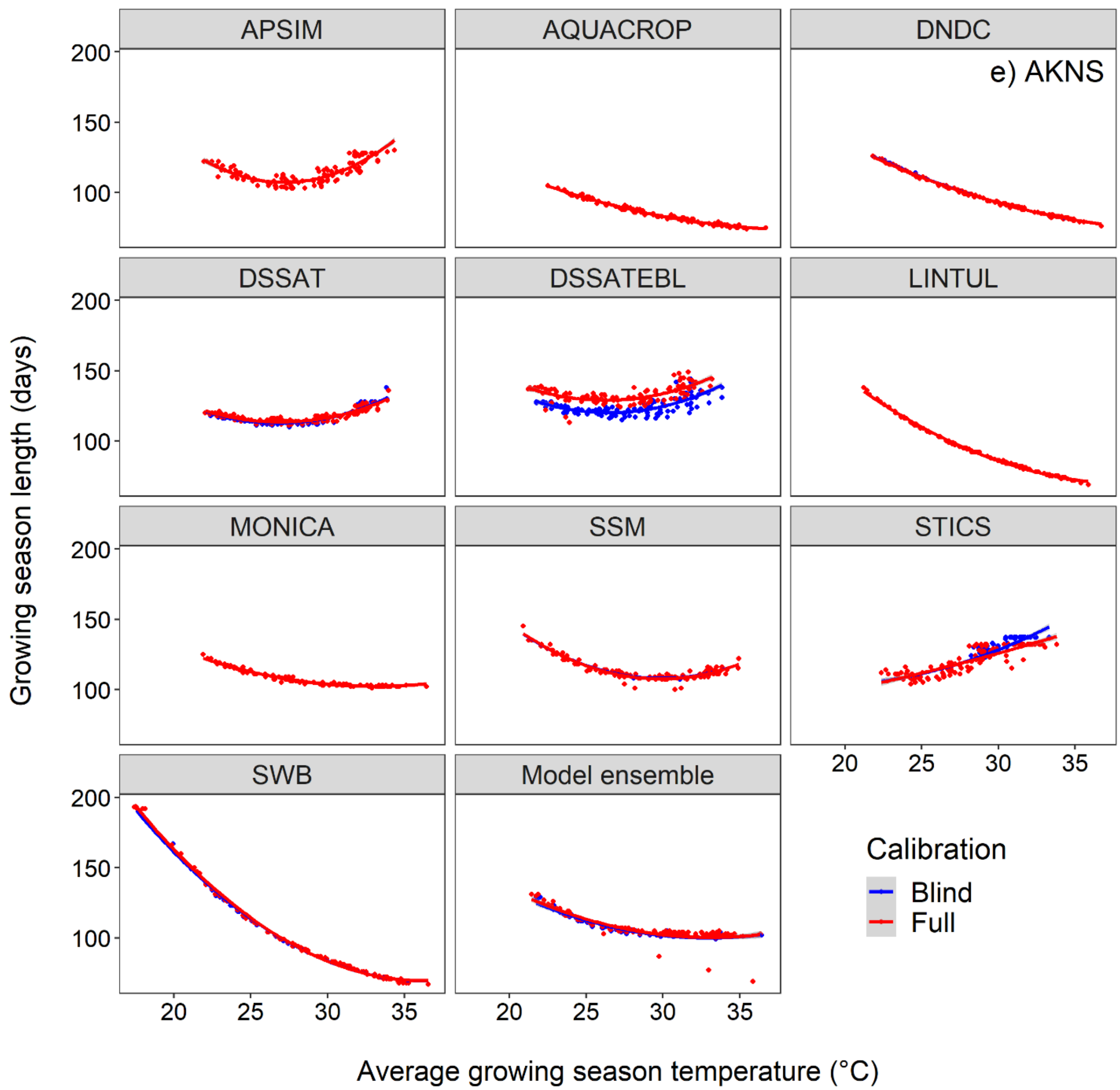

Supplementary Figure 4e. Relationship between simulated growing season length (days) and growing season temperature by model in **Arkansas**. Data plotted includes simulated yield across 30 years and temperature modification of 0, +3, +6, and +9°C from the baseline. The circles show simulated values while the lines are quadratic curves fitted using the "stat_smooth" function and "lm" method in R version 4.0.2 using a quadratic model.

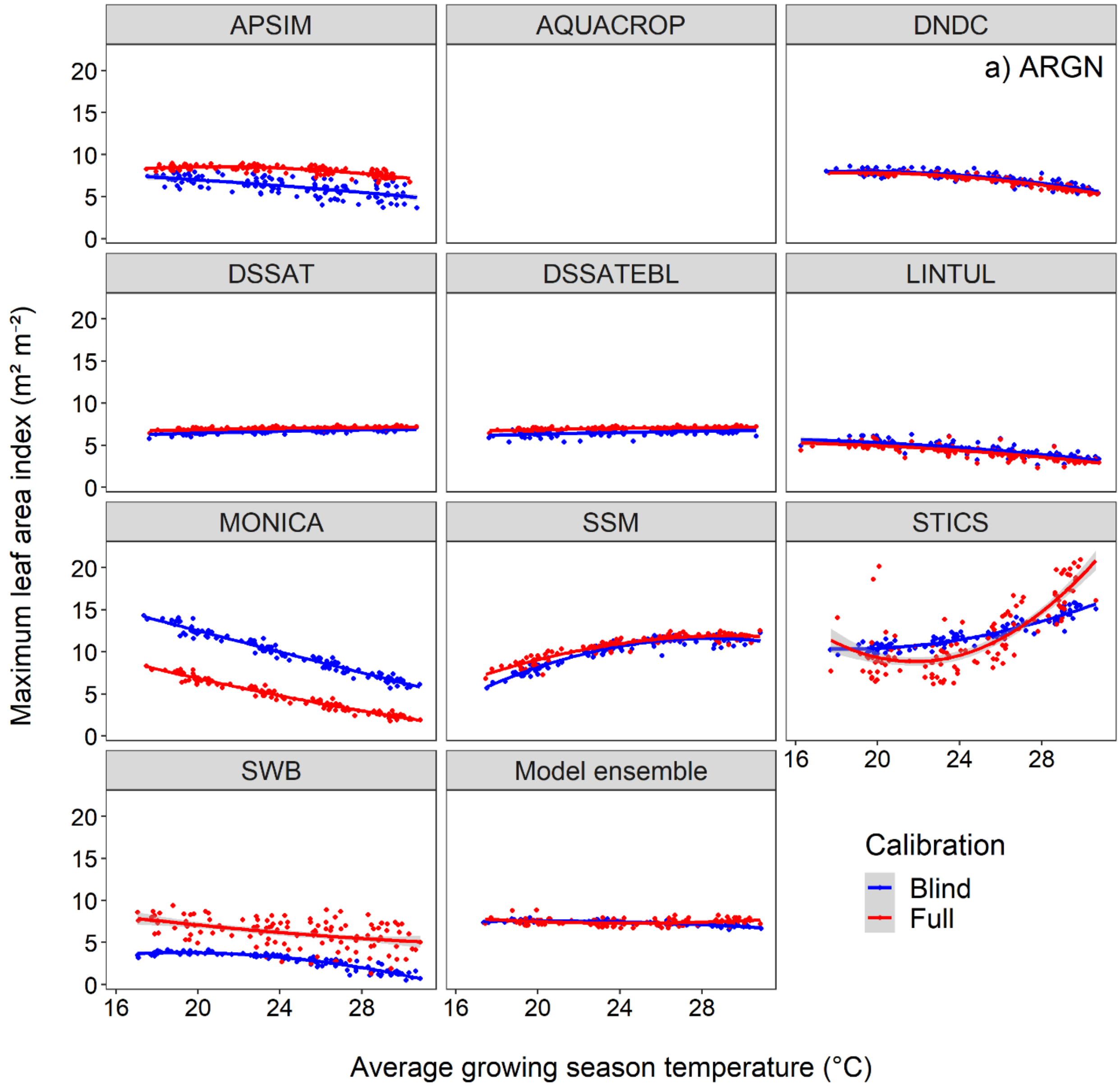

Supplementary Figure 5a. Relationship between simulated maximum leaf area index (m^2 m^{-2}) and growing season temperature by model in **Argentina**. Data plotted includes simulated yield across 30 years and temperature modification of 0, +3, +6, and +9°C from the baseline. The circles show simulated values while the lines are quadratic curves fitted using the "stat_smooth" function and "lm" method in R version 4.0.2 using a quadratic model.

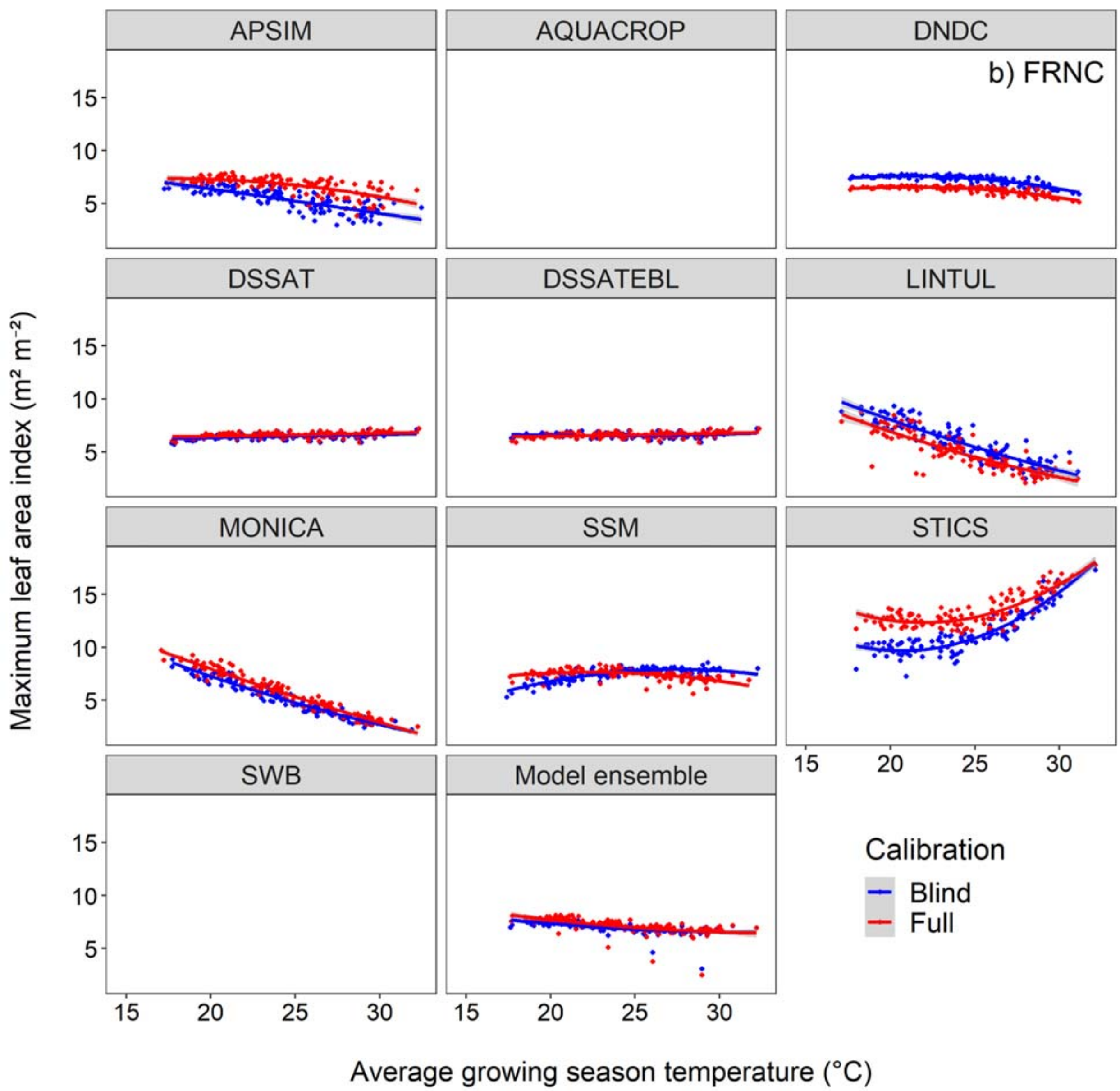

Supplementary Figure 5b. Relationship between simulated maximum leaf area index (m^2 m^{-2}) and growing season temperature by model in **France**. Data plotted includes simulated yield across 30 years and temperature modification of 0, +3, +6, and +9°C from the baseline. The circles show simulated values while the lines are quadratic curves fitted using the "stat_smooth" function and "lm" method in R version 4.0.2 using a quadratic model.

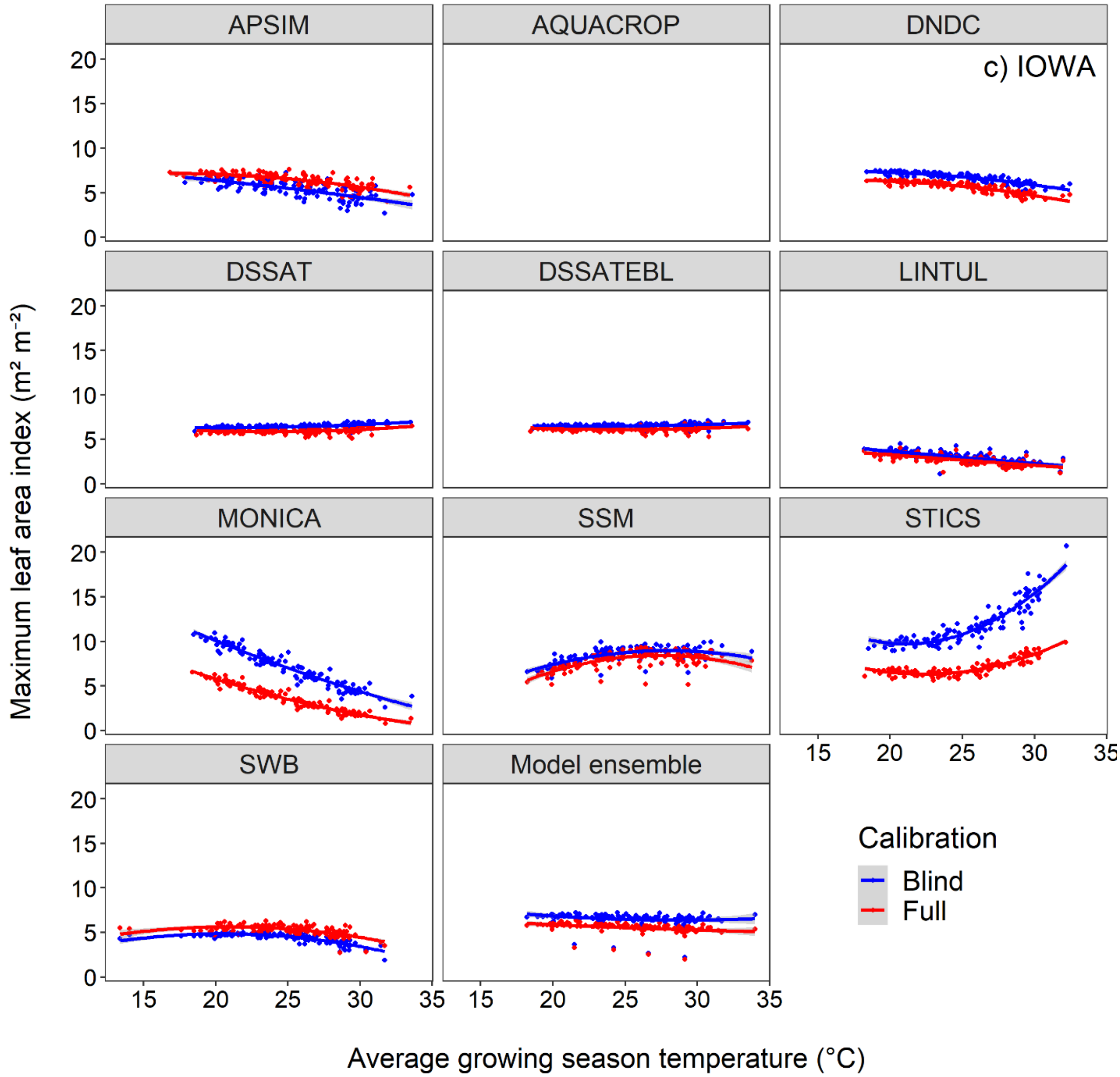

Supplementary Figure 5c. Relationship between simulated maximum leaf area index (m^2 m^{-2}) and growing season temperature by model in **Iowa**. Data plotted includes simulated yield across 30 years and temperature modification of 0, +3, +6, and +9°C from the baseline. The circles show simulated values while the lines are quadratic curves fitted using the "stat_smooth" function and "lm" method in R version 4.0.2 using a quadratic model.

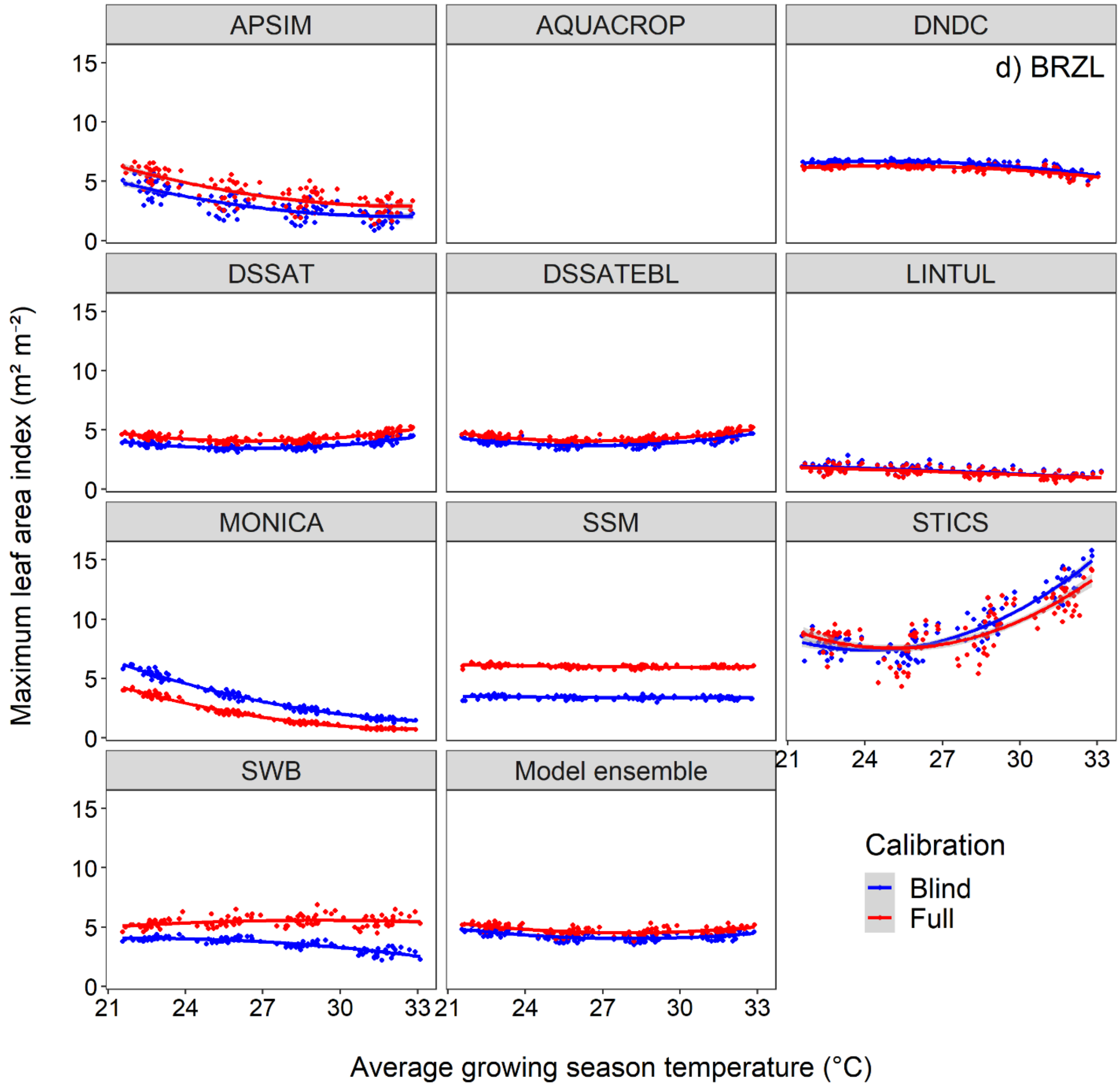

Supplementary Figure 5d. Relationship between simulated maximum leaf area index (m^2 m^{-2}) and growing season temperature by model in **Brazil**. Data plotted includes simulated yield across 30 years and temperature modification of 0, +3, +6, and +9°C from the baseline. The circles show simulated values while the lines are quadratic curves fitted using the "stat_smooth" function and "lm" method in R version 4.0.2 using a quadratic model.

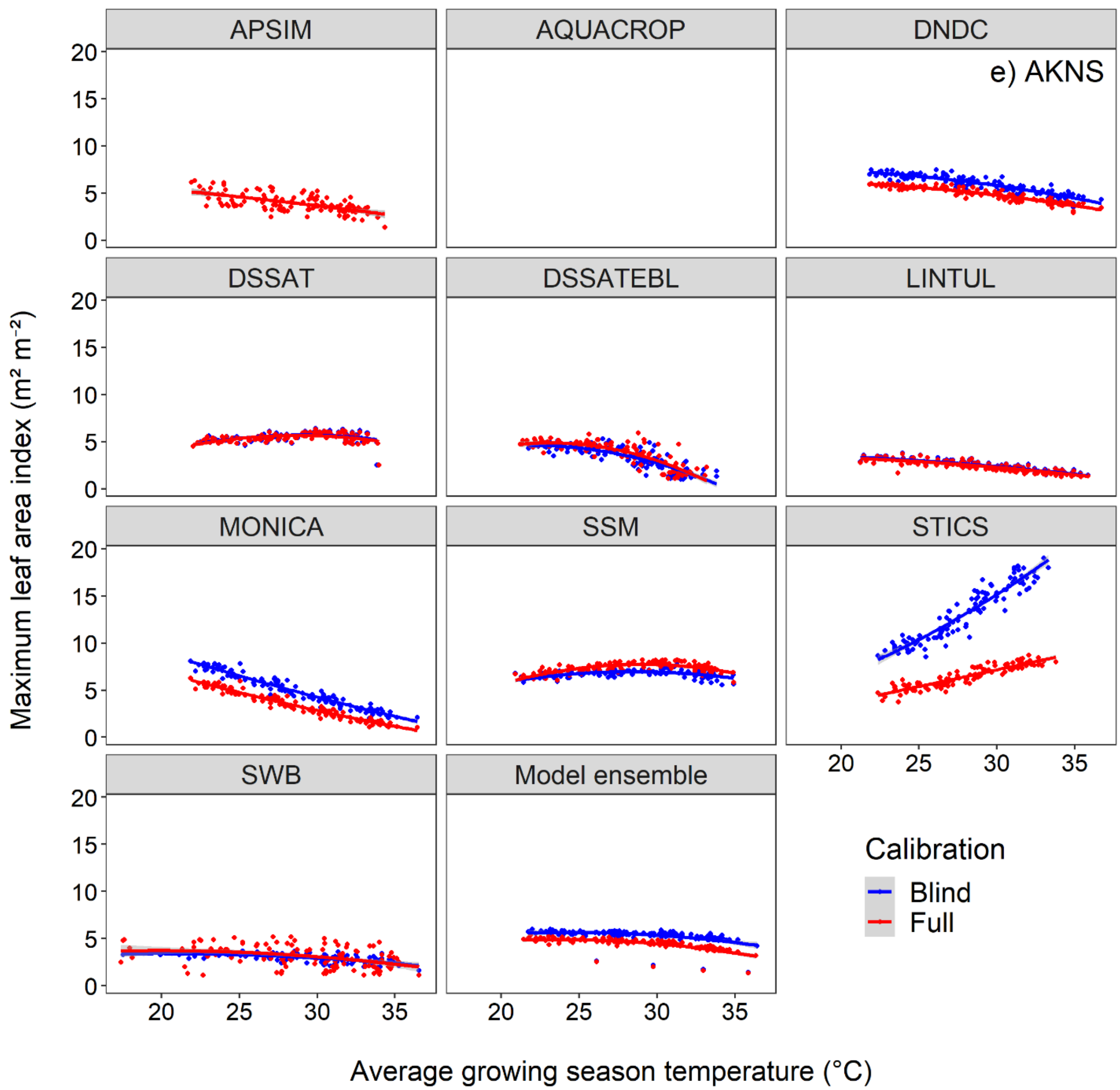

Supplementary Figure 5e. Relationship between simulated maximum leaf area index (m^2 m^{-2}) and growing season temperature by model in **Arkansas**. Data plotted includes simulated yield across 30 years and temperature modification of 0, +3, +6, and +9°C from the baseline. The circles show simulated values while the lines are quadratic curves fitted using the "stat_smooth" function and "lm" method in R version 4.0.2 using a quadratic model.

References

Ainsworth, E. A., Davey, P. A., Bernacchi, C. J., Dermody, O. C., Heaton, E. A., Moore, D. J., Morgan, P. B., Naidu, S. L., Yoo Ra, H.-s., Zhu, X.-g., Curtis, P. S., & Long, S. P. (2002). A meta-analysis of elevated [CO2] effects on soybean (Glycine max) physiology, growth and yield. *Global Change Biology 8*(8), 695-709. https://doi.org/10.1046/j.1365-2486.2002.00498.x

Allen, L. H., Zhang, L., Boote, K. J., & Hauser, B. A. (2018). Elevated temperature intensity, timing, and duration of exposure affect soybean internode elongation, mainstem node number, and pod number per plant. *The Crop Journal, 6*(2), 148-161. https://doi.org/10.1016/j.cj.2017.10.005

Alsajri, F. A., Wijewardana, C., Irby, J. T., Bellaloui, N., Krutz, L. J., Golden, B., Gao, W., & Reddy, K. R. (2020). Developing functional relationships between temperature and soybean yield and seed quality. *Agronomy Journal 112*(1), 194-204. https://doi.org/10.1002/agj2.20034

Annandale, J. G., Campbell, G. S., Olivier, F. C., & Jovanovic, N. Z. (2000). Predicting crop water uptake under full and deficit irrigation: An example using pea (Pisum sativum L. cv. Puget). *Irrigation Science, 19*(2), 65-72. 10.1007/s002710050002

Baek, J.-K., Sang, W.-G., Kim, J.-H., Shin, P., Cho, J.-I., & Seo, M.-C. (2020). Yield response of soybean [Glycine max (L.) Merrill] to high temperature cCondition in a temperature gradient chamber. *Korean Journal of Crop Science, 65*(4), 339-345. https://doi.org/10.7740/kjcs.2020.65.4.339

Baker, J. T., Allen Jr, L. H., Boote, K. J., Jones, P., & Jones, J. W. (1989). Response of Soybean to Air Temperature and Carbon Dioxide Concentration. *Crop Science 29*(1), 98-105. https://doi.org/10.2135/cropsci1989.0011183X002900010024x

Bassu, S., Brisson, N., Durand, J.-L., Boote, K., Lizaso, J., Jones, J. W., Rosenzweig, C., Ruane, A. C., Adam, M., Baron, C., Basso, B., Biernath, C., Boogaard, H., Conijn, S., Corbeels, M., Deryng, D., De Sanctis, G., Gayler, S., Grassini, P., Hatfield, J., Hoek, S., Izaurralde, C., Jongschaap, R., Kemanian, A. R., Kersebaum, K. C., Kim, S.-H., Kumar, N. S., Makowski, D., Müller, C., Nendel, C., Priesack, E., Pravia, M. V., Sau, F., Shcherbak, I., Tao, F., Teixeira, E., Timlin, D., & Waha, K. (2014). How do various maize crop models vary in their responses to climate change factors? *Global Change Biology 20*(7), 2301–2320. https://doi.org/10.1111/gcb.12520

Battisti, R., Parker, P. S., Sentelhas, P. C., & Nendel, C. (2017a). Gauging the sources of uncertainty in soybean yield simulations using the MONICA model. *Agricultural Systems, 155*, 9-18. https://doi.org/10.1016/j.agsy.2017.04.004

Battisti, R., Sentelhas, P. C., & Boote, K. J. (2017b). Inter-comparison of performance of soybean crop simulation models and their ensemble in southern Brazil. *Field Crops Research, 200*, 28–37. https://doi.org/10.1016/j.fcr.2016.10.004

Battisti, R., Sentelhas, P. C., & Boote, K. J. (2018). Sensitivity and requirement of improvements of four soybean crop simulation models for climate change studies in Southern Brazil. *International Journal of Biometeorology 62*(5), 823–832. https://doi.org/10.1007/s00484-017-1483-1

Bishop, K. A., Betzelberger, A. M., Long, S. P., & Ainsworth, E. A. (2015). Is there potential to adapt soybean (Glycine max Merr.) to future [CO_2]? An analysis of the yield response of

18 genotypes in free-air CO_2 enrichment. *Plant, Cell & Environment, 38*(9), 1765–1774. https://doi.org/10.1111/pce.12443
Boote, K. J., Allen, L. H., Prasad, P. V. V., Baker, J. T., Gesch, R. W., Snyder, A. M., Pan, D., & Thomas, J. M. G. (2005). Elevated Temperature and CO_2 Impacts on Pollination, Reproductive Growth, and Yield of Several Globally Important Crops. *Journal of Agricultural Meteorology 60*(5), 469–474. https://doi.org/10.2480/agrmet.469
Boote, K. J., Jones, J. W., Hoogenboom, G., & Pickering, N. (1998). Simulation of crop growth: CROPGRO model. In R. M. Peart & R. B. Curry (Eds.), *Agricultural systems modeling and simulation* (Vol. 18, pp. 651–692). Boca Raton, FL, USA: CRC Press.
Brisson, N., Gary, C., Justes, E., Roche, R., Mary, B., Ripoche, D., Zimmer, D., Sierra, J., Bertuzzi, P., Burger, P., Bussière, F., Cabidoche, Y. M., Cellier, P., Debaeke, P., Gaudillère, J. P., Hénault, C., Maraux, F., Seguin, B., & Sinoquet, H. (2003). An overview of the crop model STICS. *European Journal of Agronomy 18*(3), 309–332. https://doi.org/10.1016/S1161-0301(02)00110-7
Brisson, N., Launay, M., Mary, B., & Beaudoin, N. (2009). *Conceptual basis, formalisations and parameterization of the STICS crop model*. Versailles, France: Editions Quae.
Burkey, K., Tisdale, R., Zobel, R., Ray, S., & Pursley, W. (2020). Interactive Effects of Elevated Ozone and Temperature on Growth and Yield of Soybean (Glycine max (L.) Merr.) under Field Conditions. *Agronomy, 10*(11), 1803. https://doi.org/10.3390/agronomy10111803
Cuadra, S. V., Kimball, B. A., Boote, K. J., Suyker, A. E., & Pickering, N. (2020). Energy balance in the DSSAT-CSM-CROPGRO model. *Agricultural and Forest Meteorology* 108241. https://doi.org/10.1016/j.agrformet.2020.108241
Gray, S. B., Dermody, O., Klein, S. P., Locke, A. M., McGrath, J. M., Paul, R. E., Rosenthal, D. M., Ruiz-Vera, U. M., Siebers, M. H., Strellner, R., Ainsworth, E. A., Bernacchi, C. J., Long, S. P., Ort, D. R., & Leakey, A. D. B. (2016). Intensifying drought eliminates the expected benefits of elevated carbon dioxide for soybean. *Nature Plants 2*(9), 16132. 10.1038/nplants.2016.132
Greenland, S. (2019). Valid P-Values Behave Exactly as They Should: Some Misleading Criticisms of P-Values and Their Resolution With S-Values. *The American Statistician, 73*(sup1), 106-114. 10.1080/00031305.2018.1529625
Hao, X., Gao, J., Han, X., Ma, Z., Merchant, A., Ju, H., Li, P., Yang, W., Gao, Z., & Lin, E. (2014). Effects of open-air elevated atmospheric CO_2 concentration on yield quality of soybean (Glycine max (L.) Merr). *Agriculture, Ecosystems & Environment, 192*, 80-84. https://doi.org/10.1016/j.agee.2014.04.002
Hatfield, J. L., Boote, K. J., Kimball, B. A., Ziska, L. H., Izaurralde, R. C., Ort, D., Thomson, A. M., & Wolfe, D. (2011). Climate impacts on agriculture: Implications for crop production. *Agronomy Journal 103*(2), 351–370. https://doi.org/10.2134/agronj2010.0303
Holzworth, D. P., Huth, N. I., deVoil, P. G., Zurcher, E. J., Herrmann, N. I., McLean, G., Chenu, K., van Oosterom, E. J., Snow, V., Murphy, C., Moore, A. D., Brown, H., Whish, J. P. M., Verrall, S., Fainges, J., Bell, L. W., Peake, A. S., Poulton, P. L., Hochman, Z., Thorburn, P. J., Gaydon, D. S., Dalgliesh, N. P., Rodriguez, D., Cox, H., Chapman, S., Doherty, A., Teixeira, E., Sharp, J., Cichota, R., Vogeler, I., Li, F. Y., Wang, E., Hammer, G. L., Robertson, M. J., Dimes, J. P., Whitbread, A. M., Hunt, J., van Rees, H., McClelland, T., Carberry, P. S., Hargreaves, J. N. G., MacLeod, N., McDonald, C.,

Harsdorf, J., Wedgwood, S., & Keating, B. A. (2014). APSIM – Evolution towards a new generation of agricultural systems simulation. *Environmental Modelling & Software 62*, 327–350. https://doi.org/10.1016/j.envsoft.2014.07.009
Hoogenboom, G., Porter, C., Boote, K., Shelia, V., Wilkens, P., Singh, U., White, J., Asseng, S., Lizaso, J., & Moreno, L. (2019). The DSSAT crop modeling ecosystem. In K. Boote (Ed.), *Advances in crop modelling for a sustainable agriculture* (pp. 173–216). Cambridge, UK: Burleigh Dodds Science Publishing.
Jovanovic, N. Z., Annandale, J. G., & Bennie, A. T. P. (2002). Calibration and validation of the SWB irrigation scheduling model for soybean [Glycine max. (L.) Merr., indeterminate cv. Wayne]. *South African Journal of Plant and Soil, 19*(4), 165-172. 10.1080/02571862.2002.10634459
Kimball, B. A., Boote, K. J., Hatfield, J. L., Ahuja, L. R., Stockle, C., Archontoulis, S., Baron, C., Basso, B., Bertuzzi, P., Constantin, J., Deryng, D., Dumont, B., Durand, J.-L., Ewert, F., Gaiser, T., Gayler, S., Hoffmann, M. P., Jiang, Q., Kim, S.-H., Lizaso, J., Moulin, S., Nendel, C., Parker, P., Palosuo, T., Priesack, E., Qi, Z., Srivastava, A., Stella, T., Tao, F., Thorp, K. R., Timlin, D., Twine, T. E., Webber, H., Willaume, M., & Williams, K. (2019). Simulation of maize evapotranspiration: An inter-comparison among 29 maize models. *Agricultural and Forest Meteorology 271*, 264-284. https://doi.org/10.1016/j.agrformet.2019.02.037
Kuhn, T., Enders, A., Gaiser, T., Schäfer, D., Srivastava, A. K., & Britz, W. (2020). Coupling crop and bio-economic farm modelling to evaluate the revised fertilization regulations in Germany. *Agricultural Systems, 177*, 102687. https://doi.org/10.1016/j.agsy.2019.102687
Menne, M. J., Durre, I., Vose, R. S., Gleason, B. E., & Houston, T. G. (2012). An overview of the Global Historical Climatology Network-daily database. *Journal of Atmospheric and Oceanic Technology 29*(7), 897–910. https://doi.org/10.1175/jtech-d-11-00103.1
Morgan, P. B., Bollero, G. A., Nelson, R. L., Dohleman, F. G., & Long, S. P. (2005). Smaller than predicted increase in aboveground net primary production and yield of field-grown soybean under fully open-air [CO_2] elevation. *Global Change Biology 11*(10), 1856-1865. https://doi.org/10.1111/j.1365-2486.2005.001017.x
Nendel, C., Berg, M., Kersebaum, K. C., Mirschel, W., Specka, X., Wegehenkel, M., Wenkel, K. O., & Wieland, R. (2011a). The MONICA model: Testing predictability for crop growth, soil moisture and nitrogen dynamics. *Ecological Modelling, 222*(9), 1614–1625. https://doi.org/10.1016/j.ecolmodel.2011.02.018
Nendel, C., Berg, M., Kersebaum, K. C., Mirschel, W., Specka, X., Wegehenkel, M., Wenkel, K. O., & Wieland, R. (2011b). The MONICA model: Testing predictability for crop growth, soil moisture and nitrogen dynamics. *Ecological Modelling, 222*(9), 1614-1625. https://doi.org/10.1016/j.ecolmodel.2011.02.018
Ruiz-Vera, U. M., Siebers, M., Gray, S. B., Drag, D. W., Rosenthal, D. M., Kimball, B. A., Ort, D. R., & Bernacchi, C. J. (2013). Global warming can negate the expected CO_2 stimulation in photosynthesis and productivity for soybean grown in the Midwestern United States. *Plant Physiology, 162*(1), 410. https://doi.org/10.1104/pp.112.211938
Sall, J. (2002). Monte Carlo calibration of distributions of partition statistics. Retrieved from https://www.jmp.com/content/dam/jmp/documents/en/white-papers/montecarlocal.pdf
Sinclair, T. R. (1986). Water and nitrogen limitations in soybean grain production I. Model development. *Field Crops Research, 15*(2), 125-141. https://doi.org/10.1016/0378-4290(86)90082-1

Smith, W., Grant, B., Qi, Z., He, W., VanderZaag, A., Drury, C. F., & Helmers, M. (2020). Development of the DNDC model to improve soil hydrology and incorporate mechanistic tile drainage: A comparative analysis with RZWQM2. *Environmental Modelling & Software 123*, 104577. https://doi.org/10.1016/j.envsoft.2019.104577

Soltani, A., & Sinclair, T. R. (2012). *Modeling physiology of crop development, growth and yield*. Wallingford, UK: CABI.

Specka, X., Nendel, C., & Wieland, R. (2015). Analysing the parameter sensitivity of the agro-ecosystem model MONICA for different crops. *European Journal of Agronomy 71*, 73-87. https://doi.org/10.1016/j.eja.2015.08.004

Steduto, P., Hsiao, T. C., Fereres, E., & Raes, D. (2012). *Crop yield response to water* (Vol. 1028): Food and Agriculture Organization of the United Nations Rome.

Steduto, P., Hsiao, T. C., Raes, D., & Fereres, E. (2009). AquaCrop—The FAO Crop Model to Simulate Yield Response to Water: I. Concepts and Underlying Principles. *Agronomy Journal 101*(3), 426–437. https://doi.org/10.2134/agronj2008.0139s

Storck, L., Cargnelutti Filho, A., Lúcio, A. D. C., Missio, E. L., & Rubin, S. d. A. L. (2010). Avaliação da precisão experimental em ensaios de competição de cultivares de soja. *Ciência e Agrotecnologia, 34*, 572–578.

Tacarindua, C. R. P., Shiraiwa, T., Homma, K., Kumagai, E., & Sameshima, R. (2013). The effects of increased temperature on crop growth and yield of soybean grown in a temperature gradient chamber. *Field Crops Research, 154*, 74-81. https://doi.org/10.1016/j.fcr.2013.07.021

Thomas, J., Boote, K., Pan, D., & Allen Jr, L. (2010). Elevated temperature delays onset of reproductive growth and reduces seed growth rate of soybean. *J. AgroCrop Sci, 1*, 19-32.

van der Laan, M., Stirzaker, R. J., Annandale, J. G., Bristow, K. L., & Preez, C. C. d. (2010). Monitoring and modelling draining and resident soil water nitrate concentrations to estimate leaching losses. *Agricultural Water Management, 97*(11), 1779-1786. https://doi.org/10.1016/j.agwat.2010.06.012

Wallach, D., Martre, P., Liu, B., Asseng, S., Ewert, F., Thorburn, P. J., van Ittersum, M., Aggarwal, P. K., Ahmed, M., Basso, B., Biernath, C., Cammarano, D., Challinor, A. J., De Sanctis, G., Dumont, B., Eyshi Rezaei, E., Fereres, E., Fitzgerald, G. J., Gao, Y., Garcia-Vila, M., Gayler, S., Girousse, C., Hoogenboom, G., Horan, H., Izaurralde, R. C., Jones, C. D., Kassie, B. T., Kersebaum, K. C., Klein, C., Koehler, A.-K., Maiorano, A., Minoli, S., Müller, C., Naresh Kumar, S., Nendel, C., O'Leary, G. J., Palosuo, T., Priesack, E., Ripoche, D., Rötter, R. P., Semenov, M. A., Stöckle, C., Stratonovitch, P., Streck, T., Supit, I., Tao, F., Wolf, J., & Zhang, Z. (2018). Multimodel ensembles improve predictions of crop–environment–management interactions. *Global Change Biology 24*(11), 5072–5083. https://doi.org/10.1111/gcb.14411

Wang, A., Lam, S. K., Hao, X., Li, F. Y., Zong, Y., Wang, H., & Li, P. (2018). Elevated CO2 reduces the adverse effects of drought stress on a high-yielding soybean (Glycine max (L.) Merr.) cultivar by increasing water use efficiency. *Plant Physiology and Biochemistry, 132*, 660-665. https://doi.org/10.1016/j.plaphy.2018.10.016

Xu, G., Singh, S. K., Reddy, V. R., Barnaby, J. Y., Sicher, R. C., & Li, T. (2016). Soybean grown under elevated CO2 benefits more under low temperature than high temperature stress: Varying response of photosynthetic limitations, leaf metabolites, growth, and seed yield. *Journal of Plant Physiology, 205*, 20-32. https://doi.org/10.1016/j.jplph.2016.08.003